Université de Montréal

Cardiologie nucléaire du 21^{ième} siècle

Nouveautés et réalités

par

François HAREL

Sciences biomédicales

Faculté de médecine

Thèse présentée à la Faculté des études supérieures
en vue de l'obtention du grade de doctorat
en sciences biomédicales

Juin, 2009

Université de Montréal
Faculté des études supérieures

Cette thèse intitulée :

Cardiologie nucléaire du 21ième siècle: Nouveautés et réalités

présentée par :
François Harel

a été évaluée par un jury composé des personnes suivantes :

Dr Bruce Allen, président-rapporteur
Dr Paul Khairy, directeur de recherche
Mme Louise Fortier, membre du jury
Dr Raymond Taillefer, examinateur externe
Dr Louis-Gilles Durand, représentant du doyen de la FES

Résumé

Les maladies cardio-vasculaires demeurent une cause majeure de mortalité et morbidité dans les sociétés développées. La recherche de déterminants prédictifs d'évènements vasculaires représente toujours un enjeu d'actualité face aux coûts croissants des dépenses reliées aux soins médicaux et à l'élargissement des populations concernées, notamment face à l'occidentalisation des pays émergeants comme l'Inde, le Brésil et la Chine. La cardiologie nucléaire occupe depuis trente ans, une place essentielle dans l'arsenal des méthodes diagnostiques et pronostiques des cardiopathies. De plus, de nouvelles percées permettront de dépister d'une façon plus précoce et précise, la maladie athérosclérotique cardiaque et périphérique chez les populations atteintes ainsi qu'en prévention primaire. Nous présenterons dans cette thèse, deux approches nouvelles de la cardiologie nucléaire.

La dysfonction endothéliale est considérée comme le signal pathologique le plus précoce de l'athérosclérose. Les facteurs de risques cardiovasculaires traditionnels atteignent la fonction endothéliale et peuvent initier le processus d'athérosclérose même en l'absence de lésion endothéliale physique. La quantification de la fonction endothéliale coronarienne comporte donc un intérêt certain comme biomarqueur précoce de la maladie coronarienne.

La pléthysmographie isotopique, méthodologie développée lors de ce cycle d'étude, permet de quantifier la fonction endothéliale périphérique, cette dernière étant corrélée à la fonction endothéliale coronarienne. Cette méthodologie est démontrée dans le premier manuscrit (*Harel et. al., Physiol Meas., 2007*). L'utilisation d'un radiomarquage des érythrocytes permet la mesure du flot artériel au niveau du membre supérieur pendant la réalisation d'une hyperémie réactive locale. Cette nouvelle procédure a été validée en comparaison à la pléthysmographie par jauge de contrainte sur une cohorte de 26 patients. Elle a démontré une excellente reproductibilité (coefficient de corrélation intra-classe =

0.89). De plus, la mesure du flot artérielle pendant la réaction hyperémique corrélait avec les mesure réalisées par la méthode de référence (r=0.87).

Le deuxième manuscrit expose les bases de la spectroscopie infrarouge comme méthodologie de mesure du flot artériel et quantification de la réaction hyperémique (*Harel et. al., Physiol Meas., 2008*). Cette étude utilisa un protocole de triples mesures simultanées à l'aide de la pléthysmographie par jauge de contrainte, radio-isotopique et par spectroscopie infrarouge. La technique par spectroscopie fut démontrée précise et reproductible quant à la mesure des flots artériels au niveau de l'avant-bras. Cette nouvelle procédure a présenté des avantages indéniables quant à la diminution d'artéfact et à sa facilité d'utilisation.

Le second volet de ma thèse porte sur l'analyse du synchronisme de contraction cardiaque. En effet, plus de 30% des patients recevant une thérapie de resynchronisation ne démontre pas d'amélioration clinique. De plus, ce taux de non-réponse est encore plus élevé lors de l'utilisation de critères morphologiques de réponse à la resynchronisation (réduction du volume télésystolique). Il existe donc un besoin urgent de développer une méthodologie de mesure fiable et précise de la dynamique cardiaque.

Le troisième manuscrit expose les bases d'une nouvelle technique radio-isotopique permettant la quantification de la fraction d'éjection du ventricule gauche (*Harel et. al. J Nucl Cardiol., 2007*). L'étude portant sur 202 patients a démontré une excellente corrélation (r=0.84) avec la méthode de référence (ventriculographie planaire). La comparaison avec le logiciel QBS (Cedar-Sinai) démontrait un écart type du biais inférieur (7.44% vs 9.36%). De plus, le biais dans la mesure ne démontrait pas de corrélation avec la magnitude du paramètre pour notre méthodologie, contrairement au logiciel alterne.

Le quatrième manuscrit portait sur la quantification de l'asynchronisme intra-ventriculaire gauche (*Harel et. al. J Nucl Cardiol, 2008*). Un nouveau paramètre tridimensionnel (CHI: contraction homogeneity index) (médiane 73.8% ; IQ 58.7% -

84.9%) permis d'intégrer les composantes d'amplitude et du synchronisme de la contraction ventriculaire. La validation de ce paramètre fut effectuée par comparaison avec la déviation standard de l'histogramme de phase (SDΦ) (médiane 28.2º ; IQ 17.5º - 46.8º) obtenu par la ventriculographie planaire lors d'une étude portant sur 235 patients. Ces quatre manuscrits, déjà publiés dans la littérature scientifique spécialisée, résument une fraction des travaux de recherche que nous avons effectués durant les trois dernières années. Ces travaux s'inscrivent dans deux axes majeurs de développement de la cardiologie du 21^{ième} siècle.

Mots-clés : endothélium, hyperémie réactive, asynchronisme cardiaque

Abstract

Cardiovascular diseases remain a major cause of mortality and morbidity in developed countries. The search for predictive determinants of vascular events represents a relevant and timely goal, considering the increasing costs of medical care and the progress in developing countries such as India, Brazil and China. Nuclear cardiology has, for 30 years, played an essential role in the diagnosis and prognosis of various cardiac and vascular diseases. Moreover, new developments will allow earlier and more specific detection of cardiac and peripheral atherosclerosis disease in affected individuals and in primary prevention. In this thesis, we will focus on advances in two major themes of nuclear cardiology.

Endothelial dysfunction is regarded as the earliest pathological markers of atherosclerosis. Traditional cardiovascular risks factors impair endothelial function and can initiate the atherosclerosis process, even in the absence of overt endothelial disruption. Quantification of coronary endothelial function is, therefore, of considerable interest as an early biomarker for coronary disease.

The radionuclide plethysmography methodology developed during the course of my doctoral studies allows the quantification of peripheral endothelial function, which has been correlated with coronary endothelial function. This methodology is detailed in the first manuscript (*Harel et. al., Physiol Meas., 2007*). The use of red blood cell radio-labeling permits arterial flow to be measured in the upper limb during local reactive hyperemia. This new procedure was validated against strain gauge plethysmography in a cohort of 26 patients with excellent reproducibility (intraclass coefficient of correlation = 0.89). Moreover, the arterial measurements of flow during the hyperemic reaction correlated well with the reference method (r=0.87).

The second manuscript exposes the basis of infrared spectroscopy as a method for measuring arterial flow and quantifying the hyperemic reaction (*Harel et. al., Physiol*

Meas., 2008). The study protocol consisted of simultaneous measurements by strain gauge, radionuclide and infrared spectroscopy plethysmography. The spectroscopy technique was shown to be precise and reproducible for forearm measurement of arterial blood flow. This novel procedure came major advantages in reducing artifacts and in its ease of use.

The second axis of my thesis relates to the analysis of cardiac contraction synchrony. Indeed, more than 30% of patients receiving resynchronization therapy do not show clinical improvement. Moreover, this non-response rate is even higher if we consider morphological criteria of resynchronization (end-systolic volume reduction). There is therefore, an urgent need to improve a methodology to reliably and precisely measure cardiac dynamics so as to identify and monitor potential responders.

The third manuscript exposes the basis of a new radionuclide technique to quantify left ventricle ejection fraction (*Harel et. al. J Nucl Cardiol., 2007*). The study of 202 patients showed an excellent correlation (r=0.84) with the reference method (planar ventriculography). The comparison with QBS software (Cedar-Sinai), showed a lower standard deviation of bias (7.44% vs 9.36%). Moreover, unlike the alternative software, the bias did not correlate with the magnitude of the ejection fraction.

The fourth manuscript relates to the quantification of the left intra-ventricular synchronism (*Harel et. al. J Nucl Cardiol, 2008*). A new three-dimensional parameter (CHI: contraction homogeneity index) (median 73.8%; IQ 58.7% - 84.9%) was defined to allow the integration of amplitude and synchrony components of ventricular contraction. Validation of this parameter was undertaken out by comparing the standard deviation of the histogram of phase (SDΦ) (median 28.2º; IQ 17.5º- 46.8º) obtained by planar ventriculography in a study of 235 patients.

These four manuscripts, already published in the specialized scientific literature, summarize a fraction of the research tasks that we have carried out during the three last years, representing two major axes of nuclear cardiology advancement in the 21st century.

Keywords : endothelium, reactive hyperemia, cardiac synchronism

Table des matières

À M. Patrick Degrasse, qui a su sublimer
mon désir de connaissance.

Remerciements

Nous remercions le Docteur Jocelyn Dupuis, notre véritable mentor en recherche. Nous remercions également le Docteur Bernard Thibault pour avoir participé à l'initiation de notre programme de recherche portant sur l'asynchronisme cardiaque. Finalement, nous remercions sincèrement le Docteur Paul Khairy pour son soutient constant et indéniable tout au cours de la réalisation de ce grade universitaire.

Introduction

Les maladies vasculaires représentent une des causes les plus importantes de mortalité et morbidité dans les populations occidentales. Se présentant souvent sous forme d'infarctus du myocarde ou d'accidents vasculaires cérébraux, ces événements aigus sont très invalidants pour les sujets, économiquement très coûteux pour la société et comportent un taux important de récidive chez les personnes touchées. La connaissance des déterminants prédictifs des ces événements vasculaires permettrait de diminuer l'incidence globale de ces maladies. Le pronostic médical ainsi que l'utilisation des ressources pourraient aussi être optimisés par le diagnostic précoce de la maladie cardiaque athérosclérotique (MCAS). Le clinicien fait face à une panoplie de tests diagnostiques et à plusieurs approches thérapeutiques allant du traitement médical jusqu'à la revascularisation chirurgicale. Chacune de ces méthodes diagnostiques et thérapeutiques possède ses propres risques et bénéfices (1). Bien qu'un traitement vigoureux des facteurs de risque diminue les événements coronariens aigus et augmente la survie, l'angiographie coronarienne et les procédures de revascularisation sont toujours utilisées à large échelle malgré les récentes démonstrations de leur non-supériorité face au traitement médical optimal de l'angine stable (2).

La cardiologie nucléaire occupe depuis 30 ans, une place déterminante dans l'évaluation cardiaque tant du point de vu diagnostic que pronostic. Elle prend origine de l'utilisation des substances radioactives à des fins d'évaluation cardiaque. Bien que la terminologie de *cardiologie nucléaire* nous apparaisse contemporaine, les premiers liens entre le monde de la physique nucléaire et la médecine datent de près d'un siècle. En effet, une des premières

applications des radio-isotopes en médecine est attribuée à Hermann Blumgart durant les années 20. Ce cardiologue utilisa le radon dissout dans une solution saline afin de mesurer le temps de transit de la circulation centrale chez une cohorte de sujets humains (3). Son équipe située à Boston poursuivit plusieurs travaux importants et demeura à l'avant-garde des technologies médicales, notamment pour le développement du cathétérisme cardiaque. Dans les années 40, Myron Prinzmetal employa une sonde à iodure de sodium afin d'enregistrer le transit de l'albumine radio-marqué dans la circulation centrale. Ce cardiologue fit des mesures de débit cardiaque, de volume sanguin pulmonaire et de temps de transit pulmonaire à l'aide de compteurs Geiger et de détecteurs à scintillations (4). En 1953, Hal O. Anger publia un manuscrit dont le sujet allait révolutionner la cardiologie nucléaire (5). Ce scientifique développa le concept de caméra-gamma (Anger camera) permettant la réalisation d'imagerie à haute résolution et selon un mode d'acquisition dynamique. Rapidement, plusieurs chercheurs de l'époque utilisèrent cette technologie pour visualiser les structures cardiaques et leurs fonctions via l'injection de traceurs marqués au ^{99m}Technétium (6-8). En 1971, Zaret et Strauss proposèrent de synchroniser l'acquisition scintigraphique au signal provenant de l'électrocardiographe (9-10). À l'aide d'un marquage isotopique des érythrocytes, ces scientifiques développèrent la ventriculographie isotopique, examen toujours utilisé de nos jours, surtout pour un suivi cardiaque précis dans certaines conditions tel que des cardiotoxicités secondaires à une chimiothérapie (11). Cet examen fut associé à l'exercice afin d'étudier la fonction régionale et globale sous stress

(12). On note donc que la cardiologie nucléaire débuta non pas par l'étude de la perfusion myocardique mais bien par l'analyse de la fonction cardiaque.

L'étude de la perfusion cardiaque a connu son essor dans les années 70 avec l'introduction du ^{201}Tl, puis dans les années 80 avec la venue des agents marqués au ^{99m}Tc (13-18). L'utilisation de ces agents, couplés à la caméra-gamma, permettait de qualifier la perfusion myocardique au repos et à l'effort. La venu d'agents stresseurs comme le dipyridamole, la dobutamine et l'adénosine ont permis d'objectiver la diminution régionale de la réserve coronarienne par comparaison directe avec les images obtenues au repos (19-24). Aujourd'hui, la perfusion myocardique représente l'examen le plus utile et le plus effectué en cardiologie nucléaire contemporaine. Une littérature extensive portant sur plus de 50 000 patients a clairement démontrée que l'étendue et la sévérité des déficits perfusionnels identifiées à l'aide de cet examen procure un prédicteur robuste de l'incidence d'événement cardiaque (25-26).

Par ailleurs, cette spécialité a su progresser de façon significative, en accord avec les développements tant du point de vue de l'instrumentation d'imagerie que du point de vue des traceurs utilisés. Au niveau de l'instrumentation, le tomographe à émission de positrons (PET-scan) possède plusieurs avantages indéniables. Premièrement, sa sensibilité de détection est meilleure que les caméras SPECT conventionnelles puisque le PET-scan est généralement composé de multiples détecteurs en conformation annulaire,

comparativement à 1-2 ou 3 détecteurs isolés pour le SPECT. La résolution spatiale du système est également supérieure, pouvant atteindre moins de 5mm (FWHM) et cette méthodologie permet une analyse quantitative des processus physiologiques. Un autre avantage indéniable à cette technologie est l'utilisation de radio-isotopes associés à des molécules simples comme le fluor, carbone, azote et oxygène. On comprend que ces éléments sont fortement utilisés en chimie organique, ouvrant la porte à des radio-marquages très appropriés en recherche médicale. Par exemple, le ^{18}F est utilisé pour marquer le deoxyglucose, et ce depuis les années 80 (27-28). Son utilisation est encore considérée comme la mesure 'gold-standard' dans l'évaluation de la viabilité myocardique.

Dans les sections suivantes, j'exposerai deux avancées récentes de la cardiologie nucléaire en mentionnant les concepts fondamentaux, la physiopathologie, l'utilité de la médecine nucléaire dans ces domaines, les approches compétitrices et mon apport dans ces deux sujets. Le premier sujet traite de la mesure non-invasive de la réactivité brachiale. Le deuxième sujet porte sur la mesure de l'asynchronisme de contraction cardiaque.

Évaluation non-invasive de la réactivité brachiale

Introduction

L'endothélium vasculaire est composé d'une couche monocellulaire tapissant la surface interne des vaisseaux sanguins et faisant contact avec la lumière vasculaire. Il possède une fonction de protection, agissant comme barrière entre l'ensemble des tissus et le sang circulant. De plus, il agit comme filtre intelligent en facilitant le passage bidirectionnel de macromolécules et gaz sanguins. Il répond également aux stimuli physiques et chimiques tels les changements hémodynamiques et les forces de cisaillement et synthétise une variété de régulateurs vasoactifs autocrines et paracrines qui sont véhiculés par le compartiment sanguin. Une relâche balancée de ces facteurs bioactifs facilite l'homéostasie vasculaire. Ces agents relaxants relâchés par l'endothélium sont regroupés sous le nom de EDRF pour 'endothelium-derived relaxing factor'. L'agent clé parmi ce groupe est l'oxyde nitrique (NO), qui est synthétisé à partir de la L-arginine sous l'influence de l'enzyme NO-synthétase (NOS). En plus d'être le déterminant majeur du tonus basal des muscles lisses vasculaires, le NO oppose son action aux multiples facteurs constrictifs dérivant eux aussi de l'endothélium tels que l'angiotensine II et l'endothéline-1 (ET-1). La dysfonction endothéliale est un terme général impliquant la diminution de la production ou de la disponibilité du NO et/ou le déséquilibre entre la contribution relative des facteurs relaxants et constricteurs dérivant de l'endothélium. Dans cette définition, le terme NO inclus plus ou moins l'ensemble des facteurs relaxants. La dysfonction endothéliale coronarienne contribue aux manifestations ischémiques de la maladie coronarienne ainsi que la progression de l'athérosclérose (29-31).

L'endothélium possède des fonctions anticoagulantes, fibrinolytiques et antiplaquettaires. Via sa fonction de régulation vasculaire, il contrôle le tonus vasculaire des muscles lisses coronariens et répond aux stimuli pharmacologiques et physiologiques (32).

Le NO maintient une vasodilatation artérielle de base qui contrecarre le tonus vasoconstricteur artériel intrinsèque présent dans la circulation coronaire, pulmonaire et systémique. Le système endothélial est donc dispersé sur l'ensemble de l'endothélium humain. Le NO est stimulé par l'augmentation de flot, qui engendre une augmentation des forces de cisaillement sur l'endothélium, stimulant en retour la relâche endothéliale. De plus, l'endothélium réagit à de nombreux agents circulants exogènes et endogènes tels que l'acétylcholine et les bradykinines.

La dysfonction endothéliale apparaît de façon précoce dans le développement de la MCAS et est associée à un pronostic défavorable par rapport aux individus ne présentant pas de dysfonction endothéliale. Des études expérimentales ont démontré qu'une atteinte physique de l'endothélium entraîne la formation de plaque athérosclérotique (29). Un bilan lipidique perturbé (LDL haut ou HDL bas), un tabagisme actif ou passif, l'hypertension et le diabète sont associés à une dysfonction endothéliale même chez les individus en santé sans évidence d'athérosclérose (33). Une histoire familiale de MCAS précoce est associée à une dysfonction endothéliale même chez le jeune adulte (34). Les mécanismes reliant les

facteurs de risque de MCAS et la dysfonction endothéliale sont encore peu connus. Par contre, on pense qu'ils sont reliés à une augmentation du stress oxydatif qui est une cause importante de dysfonction endothéliale.

Bien que représentant une phase asymptomatique à l'intérieur d'un continum physiopathologique, la dysfonction endothéliale est un précurseur direct de la coronaropathie athérosclérotique. Cliniquement, cette dernière entité se manifeste par 1) le vasospasme, 2) la formation de thrombus, 3) l'hypertension et 4) l'athérosclérose (35). La dysfonction endothéliale cause aussi une diminution de production de NO ainsi qu'une diminution de la biodisponibilité locale du NO. On comprend que la diminution de NO augmente l'athérosclérose par vasoconstriction locale, augmentation de l'adhérence et de l'agrégation plaquettaire et augmentation de la prolifération des cellules musculaires lisses (36). L'effet de vasodilatation de la fonction endothéliale sur la microcirculation myocardique est un déterminant important de la perfusion myocardique durant les périodes où le travail myocardique est augmenté. La dysfonction endothéliale de la microcirculation joue donc un rôle significatif dans la pathogenèse de l'ischémie myocardique (37). Plusieurs études ont démontré que les hypolipémiants oraux diminuent l'ischémie (38-44) et améliore la survie chez les patients avec MCAS (45) malgré une faible régression des plaques mesurées par angiographie coronarienne (46). Ce bénéfice est probablement associé à une amélioration de la fonction endothéliale.

La dysfonction endothéliale est associée à une augmentation significative de l'incidence d'événements cardiovasculaires durant un suivi à long terme. Pour cette raison, un intérêt grandissant existe envers les méthodes permettant d'évaluer la fonction endothéliale chez les individus et servant d'aide à la stratification de la maladie cardiovasculaire ou comme outil de dépistage précoce chez les patients asymptomatiques. Dans les prochains paragraphes, j'exposerai les différentes méthodes d'évaluation de la fonction endothéliale.

Méthodes d'évaluation non-isotopiques de la fonction endothéliale

Angiographie coronarienne

Cette méthode est utilisée pour évaluer la fonction endothéliale coronarienne depuis 1986 (47). Le diamètre des artères coronaires est mesuré avant et après injection d'acétylcholine qui stimule la relâche de NO endogène des cellules endothéliales, provoquant une vasodilatation chez les sujets avec fonction endothéliale préservée. Chez les sujets atteints de dysfonction endothéliale, l'acétylcholine agit directement sur les muscles lisses vasculaires entraînant une vasoconstriction paradoxale en l'absence de réaction endothéliale opposée. Initialement, cette technique a permis de mieux connaître les facteurs de risque de la dysfonction endothéliale dans les artères coronaires (48) et de découvrir que celle-ci initie l'athérosclérose coronarienne (29). Les désavantages de cette technique sont

sa nature invasive, l'exposition aux radiations et la nécessité d'utiliser des logiciels poussés d'analyse d'images.

Pléthysmographie par occlusion veineuses

La dysfonction endothéliale peut être considérée comme une pathologie systémique ce qui permet son évaluation au niveau des vaisseaux périphériques. L'infusion de vasodilatateurs endothélial-dépendant et indépendant au niveau de l'artère brachiale permet l'évaluation de la fonction endothéliale au niveau de la microcirculation de l'avant-bras en mesurant le flot artériel à l'aide de la pléthysmographie d'impédance par occlusion veineuse (49-50). L'utilisation de différentes substances vaso-actives stimulant ou inhibant la relâche de NO permet de bien caractériser la fonction endothéliale endogène. Les désavantages de cette méthode incluent sa nature légèrement invasive par la nécessité de canuler l'artère brachiale et le fait que les mesures soient effectuées sur les vaisseaux périphériques.

Plus récemment, on a remplacé l'injection intra-artérielle par la technique d'hyperémie réactive (51), un test de provocation utilisé pour évaluer la réserve circulatoire en réponse à un stimulus ischémique. Cette technique utilise la création d'une ischémie temporaire au niveau du membre supérieur ce qui entraîne une diminution importante des résistances en aval de l'occlusion. Lors de la relâche de l'ischémie, le flot artériel est transitoirement augmenté jusqu'à ce qu'un état d'équilibre soit de nouveau atteint. Durant la phase transitoire, l'augmentation de flot engendre des forces de cisaillement sur l'endothélium des

vaisseaux de conductances provoquant une relâche de peptides vaso-actifs dont le NO (52). Ces peptides vont moduler temporairement les réactions de l'ensemble des vaisseaux locaux situés en aval des sites de relâche et donc augmenter eux aussi le flot artériel transitoire via une vasodilatation endothélium-dépendante. La quantité de peptide relâchée est fonction de l'état de l'endothélium, ce qui permet de qualifier la fonction endothéliale.

IVUS, Doppler guidewire et pressure guidewire

D'autres méthodes telles que l'échographie intra-coronarien (IVUS), les études Doppler et les mesures directes des pressions intra-coronariennes, ont été utilisées dans quelques études mais n'ont pas connu une diffusion significative étant donnée la lourdeur technique de ces méthodes (53-56). De plus, toutes ces techniques ne peuvent être utilisées que lors d'une angiographie coronarienne.

Résonance magnétique cardiaque

La résonance magnétique fonctionnelle permet d'évaluer simultanément le diamètre des sténoses coronariennes et la mesure de la perfusion coronarienne (57-59). Elle utilise une méthode de premier passage avec agent de contraste ferromagnétique. Bien que techniquement très intéressante, il s'agit encore d'une technique limitée à la recherche de par la faible disponibilité de l'appareillage. De plus, certains problèmes restent à résoudre comme la suppression des mouvements respiratoires.

Échographie brachiale

Cette méthode mesure les variations de diamètre des vaisseaux de conductances de l'avant-bras en réponse à une augmentation des forces de cisaillement causée par une hyperémie réactive. Dans ce contexte, la vasodilatation brachiale est causée principalement par une relâche de NO endothéliale (60). Cette méthode a été utilisée chez plusieurs populations telles que des sujets jeunes et a démontré sa capacité à qualifier la présence de dysfonction endothéliale chez de jeunes sujets asymptomatiques possédant des facteurs de risque tels que l'hypercholestérolémie ou le tabagisme. Les désavantages de cette procédure sont la difficulté technique d'obtenir des données valides et des problèmes d'utilisation à large échelle qui sont reliés à une faible reproductibilité intra et inter-centres.

Tonométrie digitale

Il s'agit d'une technique relativement nouvelle qui analyse de façon non-invasive l'onde de pression artérielle périphérique. La tonométrie était déjà utilisée en médecine au niveau de l'œil pour mesurer les pressions intra-occulaires. La précision de cette technique a été validée chez l'animal et l'humain et cette modalité se prête bien à un usage large étant donné son caractère non-invasif (61-65). Par analyse de la forme de la courbe cyclique de pression artérielle, on parvient à observer les variations de flot produites par l'administration de substances vasoactives. On suppose donc que ces variations sont

fonction de l'état du système endothélial d'où la possibilité d'évaluer ce dernier (66-68). Cette méthode pourrait représenter un choix judicieux pour la mesure non-invasive de la fonction endothéliale. Par contre, des recherches restent à faire afin de valider la reproductibilité intra et inter-observateur.

Méthodes isotopiques d'évaluation de la fonction endothéliale

Tomographie par émission de positron

Ce système d'imagerie permet de quantifier de façon absolue la perfusion myocardique au repos et après stimulation pharmacologique, permettant la mesure de la réserve coronarienne. De récentes études ont démontré une réduction de la réserve coronarienne dans des territoires sans MCAS chez des patients ayant des atteintes vasculaires dans d'autres vaisseaux coronariens. De plus, la réserve coronarienne est diminuée chez des patients asymptomatiques présentant une hypercholestérolémie, un diabète ou de l'hypertension (69-75). Ces découvertes suggèrent que la diminution de la réactivité coronarienne est un marqueur précoce de la dysfonction endothéliale associée à la MCAS. Malheureusement, l'accessibilité à cet appareillage demeure encore limitée.

Tomographie d'émission monophotonique

Utilisant un appareillage plus répandu, cette technologie utilise des isotopes radioactifs permettant de mesurer la réserve perfusionnelle relative en comparant la perfusion des

territoires ischémiques aux régions présumées normalement perfusées. Comme la MCAS et la dysfonction endothéliale touchent probablement de façon diffuse les vaisseaux coronariens, l'évaluation de la réserve perfusionelle ne permet pas d'identifier les atteintes précoces (76-77) car il s'agit d'une quantification relative et aucune certitude n'existe au sujet de la normalité perfusionelle des régions présumées saines. On peut quand même penser que cette technique est plus spécifique pour l'évaluation ischémique que les méthodes purement anatomiques comme l'angiographie coronarienne simple. En effet, des études ont démontré une diminution significative de l'augmentation du flot coronarien après injection d'acétylcholine mesurée par Doppler guidewire pour les patients ayant des déficits réversibles au dipyridamole et ce même en l'absence de lésion significative à l'angiographie simple (77). De plus, le SPECT a démontré une amélioration des déficits perfusionnels chez des patients avec lésions coronariennes significatives où un traitement agressif des facteurs de risque avait été instauré (39, 43-44). D'autres études ont démontré la normalisation des déficits réversibles après administration per os de L-arginine, cette molécule améliorant probablement la perfusion myocardique via l'augmentation de la production de NO (78).

Analyse de l'hyperémie réactive

Cette technique a déjà été utilisée pour mesurer de façon non-invasive les flots artériels périphériques en marquant différentes populations cellulaires à l'aide de radio-isotopes (79-80). Elle servait principalement soit dans le cadre de recherches fondamentales ou comme

outil permettant d'évaluer les patients atteints d'athérosclérose périphérique oblitérante. Récemment, nous avons collaboré à une étude sur l'analyse du flot brachial par étude isotopique lors d'une hyperémie réactive (81). Cette recherche étudiait le passage d'un bolus compact de radiotraceur au niveau de l'avant-bras post hyperémie réactive. Cette étude a été réalisée chez deux groupes de patients dont l'un possédait plusieurs facteurs de risque de MCAS donc une haute probabilité de dysfonction endothéliale. Le deuxième groupe était composé de patients avec un faible risque de MCAS. Les résultats préliminaires démontrent que l'analyse des courbes du passage du bolus aux niveaux des membres supérieurs possède un assez bon pouvoir prédicteur de l'appartenance du groupe à haut risque de dysfonction endothéliale (sensibilité de 0.70 et spécificité de 0.60).

Bien que les résultats soient encourageants, cette étude laisse plusieurs questions en suspens. Premièrement, le critère prédictif est calculé à partir du ratio de pente représentant l'arrivée du traceur aux niveaux des membres supérieurs gauche et droit. Les analyses statistiques révèlent que seule la pente du bras controlatéral à l'hyperémie réactive démontre une différence significative entre les deux groupes. Le caractère prédictif du ratio est donc relié à l'effet de l'hyperémie sur le bras controlatéral. À notre connaissance, aucune recherche n'a exploré cet effet à distance de la relâche d'ischémie. De plus, de par le caractère compact du radiotraceur, seul une analyse transitoire des phénomènes est possible. Comme les variations hémodynamiques lors de l'ischémie, mais surtout après

l'ischémie sont elles-même transitoires, l'analyse s'en trouve par le fait même imparfaite et limitée.

Pléthysmographie isotopique

Cette technique, développée dans notre laboratoire, se base sur la méthodologie de la pléthysmographie par occlusions veineuses répétées. En effet, une compression à l'aide d'un brassard gonflé à 50 mmHg provoque une occlusion veineuse tout en maintenant une circulation artérielle intacte. Ce faisant, il se produit un accroissement de volume dans la zone située en aval au site de compression. Cet accroissement est proportionnel au flot artériel entrant dans la zone d'étude. L'augmentation de volume peut être mesurée par une jauge d'étirement (*strain gauge plethtysmography*). Dans notre cas, l'utilisation d'un marquage autologue des érythrocytes a permis d'obtenir un signal radioactif proportionnel au nombre de globules rouges séquestrés dans la zone d'étude. La répétition d'un cycle d'occlusions veineuses et de relâches permet des mesures séquentielles du flot artériel. Ce flot artériel peut être modulé par l'injection d'agents vaso-actifs, ou comme dans notre programme de recherche, par l'utilisation d'une hyperémie réactive.

Contrairement à la méthode de flot brachial, la pléthysmographie isotopique permet d'obtenir une multiplicité de mesures de flots artériels durant l'hyperémie réactive ce qui bonifie les données obtenues lors de l'expérimentation et accroît notre capacité de compréhension et d'analyse des phénomènes observés.

Asynchronisme de contraction cardiaque

Introduction

L'insuffisance cardiaque est un syndrome clinique résultant d'un désordre structurel ou fonctionnel qui diminue la capacité de la pompe cardiaque à s'adapter aux modifications de débit commandées par les variations du métabolisme corporel. Ce défaut d'adaptation est associé à un désordre dans le remplissage ventriculaire et/ou dans sa capacité à éjecter son contenu sanguin. Les principaux symptômes associés à ce syndrome sont la diminution de la tolérance à l'effort, la rétention liquidienne, la dyspnée et la fatigue. Plusieurs substrats pathophysiologiques peuvent être à l'origine de ce syndrome tels que les troubles du rythme, les atteintes péricardiques ou myocardiques, les valvulopathies et les anomalies touchant les grands vaisseaux.

Connaissances actuelles

Ce syndrome touche environ 450 000 personnes aux Canada avec une incidence annuelle de 50 000 cas et est la cause la plus importante d'hospitalisation chez les gens de plus de 65 ans (82-83). Malgré la diminution de la mortalité cardiovasculaire depuis les trois dernières décades, la prévalence de l'insuffisance cardiaque n'a cessé d'augmenter. De nouveaux traitements efficaces pour l'infarctus du myocarde, les maladies valvulaires, l'hypertension et les arythmies ventriculaires ont eu comme effets d'augmenter le nombre de patients survivant à la pathologie primaire, mais présentant aussi une dysfonction ventriculaire gauche et des manifestations cliniques d'insuffisance cardiaque. Cette

pathologie comporte une morbidité élevée et diminue la qualité de vie et la capacité fonctionnelle des patients atteints. De plus, elle contribue à une augmentation importante du risque de mortalité et ces patients nécessitent des hospitalisations plus fréquentes contribuant à une hausse des coûts du système de santé (84).

Insuffisance cardiaque et asynchronisme

L'insuffisance cardiaque est généralement causée par une perte de la masse effective du myocarde, souvent initiée par un infarctus. En plus d'observer une perte de la contractilité globale, la pathologie est souvent associée à des troubles de conduction qui aggravent le déficit hémodynamique caractéristique de l'insuffisance cardiaque (85-88).

Ces anomalies de conductions peuvent engendrer un asynchronisme auriculo-ventriculaire, un délai de conduction interventriculaire avec activation non-simultanée des deux ventricules ainsi qu'un défaut de conduction intra-ventriculaires affectant la séquence d'activation et de relaxation du ventricule gauche. L'importance de l'asynchronisme intra-ventriculaire chez les patients avec insuffisance cardiaque a été démontrée par l'association entre le pronostic et la durée du QRS (89). Les troubles de conductions intra-ventriculaires sont fréquemment observés chez les patients avec insuffisance cardiaque sévère, survenant chez plus de 40% de ces patients. Généralement, un bloc de branche gauche est présent, causant un délai d'activation du ventricule gauche par rapport au ventricule droit.

Ce bloc de branche gauche a des effets hémodynamiques négatifs en réduisant la fonction cardiaque (85, 88) et est un prédicteur indépendant d'événement cardiaque aigu chez les patients porteurs d'insuffisance cardiaque (89). Il a aussi été identifié comme un marqueur de la progression de la cardiomyopathie (90). L'activation électrique tardive du ventricule gauche retarde la contraction de sa paroi latérale malgré une contraction normale de sa paroi septale causant un désavantage mécanique qui aggrave la dysfonction systolique préexistante. La combinaison à un mouvement anormal du septum entraîne une détérioration du volume ventriculaire et de la fraction d'éjection (85-87, 91-92). D'ailleurs, dans de rares cas où des changements hémodynamiques surviennent durant un bloc de branche gauche intermittent, on a rapporté une diminution du dP/dt, du débit cardiaque, de la pression artérielle moyenne et de la fraction d'éjection globale. Dans des cas très sévères, une régurgitation mitrale pré-systolique peut aussi survenir. Les troubles de conductions peuvent aussi entraîner des effets additionnels tels que des anomalies de perfusion et du métabolisme myocardique (93-94).

Stimulation cardiaque

Des études ont démontré que la stimulation à l'apex du ventricule droit engendre un asynchronisme intraventriculaire gauche qui est délétère pour ledit ventricule. Les effets sont similaires à ceux retrouvés chez les sujets ayant un bloc de branche gauche. (95-98).

Depuis les dernières années, des avancements majeurs ont été effectués pour traiter l'insuffisance cardiaque entre autre, le développement de cliniques multidisciplinaires, l'avenue de nouveaux agents pharmacologiques et de dispositifs implantables. Également, de récentes études cliniques ont démontré que les défibrillateurs implantables (ICD) prolongent la survie chez les patients avec un antécédent d'arythmies ventriculaires malignes ou d'infarctus du myocarde combiné à une dysfonction ventriculaire gauche (99-104). L'impact majeur de cette thérapie sur la mortalité se retrouve surtout chez les patients avec dysfonction ventriculaire gauche (101). Malheureusement, bien que les défibrillateurs standards diminuent la mortalité, il n'améliore pas la capacité fonctionnelle ni la qualité de vie chez les patients présentant une insuffisance cardiaque.

Thérapie de resynchronisation cardiaque

Il y a plus de 10 ans, des études suggéraient qu'une stimulation double-chambres puisse aider cette classe de patients atteints de défaillance cardiaque, surtout pour ceux présentant un intervalle PR très allongé à l'électrocardiogramme (ECG) de base (105), possiblement parce qu'une contraction auriculaire mieux synchronisée améliore le remplissage diastolique du ventricule gauche. Cette technique fut appelée *thérapie de resynchronisation cardiaque* (TRC). Depuis, l'indication des électrostimulateurs s'est élargie aux patients atteints d'insuffisance cardiaque. Ces appareils augmentent la survie chez les patients bénificiant d'une thérapie médicale optimale pour traiter leur cardiomyopathie mais

présentant toujours des symptômes d'insuffisance cardiaque (106-107). Ces patients doivent présenter les critères de sélection suivants:

- Insuffisance ventriculaire sévère (classe NYHA 3 ou 4)
- Fraction d'éjection ventriculaire gauche < 35%
- Conduction ventriculaire anomale (QRS > 120ms)

Les manufacturiers ont développé des stimulateurs cardiaques comportant des électrodes permettant d'exciter les deux ventricules de façon autonome afin de corriger l'asynchronisme inter-ventriculaire. La TRC est donc une technique permettant d'optimiser les délais AV, intra et inter-ventriculaire chez les patients présentant les critères de sélection (108-109). On a récemment démontré qu'elle améliore les symptômes, la tolérance à l'exercice, la qualité de vie (QOL), diminue le remodelage ventriculaire et augmente la fraction d'éjection chez les patients sélectionnés (106, 110-111).

Non-réponse à la thérapie de resynchronisation

La TRC a un bénéfice global certain auprès des populations étudiées, diminue le besoin d'hospitalisation et réduit la mortalité de toutes causes (106-107). Cependant, les études cliniques ont démontré que ces gains étaient absents chez plus de 30% des patients traités avec une TRC (107, 112). Évidemment, les critères de réponse à la TRC méritent d'être

standardisés afin de mieux préciser l'efficacité réelle de cette thérapie. À ce titre, de nombreux auteurs proposent d'utiliser le critère de remodelage inverse comme point d'aboutissement de futures études (111-114). Ceci implique une précision dans la mesure du volume ventriculaire suffisante pour permettre des comparaisons volumétriques répétées. Plusieurs études suggèrent qu'une réponse clinique précoce favorable est habituellement associée à une diminution du remodelage ventriculaire à court terme (3 mois). On suggère donc pour la TRC, une période d'essai clinique de 1-3 mois avant de pouvoir déterminer le succès ou l'échec de la resynchronisation (115).

Les efforts pour prédire la réponse des patients à la resynchronisation et comprendre les raisons de l'absence d'amélioration tendent vers des résultats conflictuels (116-120). De façon étonnante, certains patients avec un QRS relativement étroit présentent une amélioration à une thérapie de resynchronisation (117-118, 121). Bien qu'en général, les patients avec un QRS large bénéficient de la resynchronisation, la corrélation entre la réduction de la durée du QRS et l'amélioration clinique est modérée et controversée (116, 122-125). De plus, la présence d'un bloc de branche gauche n'est pas toujours associée à un asynchronisme ventriculaire gauche sévère (121). Certaines études ont suggéré que la stimulation uni-ventriculaire gauche, sans diminution de la durée du QRS, engendre une amélioration similaire ou même meilleure que la stimulation bi-ventriculaire (126-131). Ceci suggère que la configuration courante de la stimulation biventriculaire ne soit pas

optimale. D'où l'intérêt de 1) bien sélectionner les patients pouvant bénéficier de la TRC et 2) optimiser les paramètres de l'appareil afin de maximiser la réponse de ces derniers.

Identification de l'asynchronisme

Il est naturel de penser qu'un patient doit présenter de l'asynchronisme afin de répondre à la thérapie de resynchronisation. En général, les patients avec un délai de conduction important présentent aussi un important asynchronisme de contraction tel que démontré par l'échocardiographie 3D, le Doppler tissulaire ou la résonance magnétique (127, 130, 132-147). Cet asynchronisme peut prendre la forme d'un délai AV anormal, ou encore d'un délai inter-ventriculaire ou intra-ventriculaire trop élevé.

Initialement, il fut supposé que l'asynchronisme auriculo-ventriculaire soit le principal facteur impliqué dans la pathogénèse des troubles de conduction associées à l'insuffisance cardiaque. Ce postulat motiva la réalisation de plusieurs études portant sur l'optimisation du délai AV. Néanmoins, des études hémodynamiques en phase aiguë ont démontré que l'impact du délai AV, dans une plage physiologique, était moins important que l'impact de la resynchronisation mécanique intra-ventriculaire (148-150). Les effets bénéfiques de la thérapie de resynchronisation, même chez des patients atteints de fibrillation auriculaire chronique, ont confirmé cette hypothèse (151-153). Il existe donc un besoin clinique dans le développement d'un outil fiable permettant de quantifier les délais ventriculaires et d'analyser la dynamique de contraction cardiaque. Ceci est d'autant plus vrai depuis les

échecs des récentes études RethinQ et PROSPECT (154-156). En effet, ces dernières études ont démontré les faiblesses importantes des techniques échocardiographiques. Bien que cette méthodologie soit d'utilité certaine et répandue, elle n'a su fournir de critères permettant de prédire de façon fiable et reproductible, la réponse à une thérapie de resynchronisation. De plus, toujours en utilisant cette modalité d'imagerie, l'étude RethinQ n'a pu démontrer un quelconque avantage à utiliser une CRT chez des patients avec QRS d'une durée inférieure à 120ms.

Ces deux derniers contre-résultats démontrent clairement que la recherche de paramètres simples, fiables et robustes demeurent encore d'actualité et nécessite d'étudier de nouvelles approches de mesures et d'analyses.

Résumé des méthodologies

Comme cette thèse porte sur deux sujets scientifiques distincts, mais intimement lié à des avancements important de la cardiologie nucléaire, nous inclurons deux publications par sujet. La première est une étude expérimentale portant sur la conception et l'utilisation d'un système mobile permettant la mesure de l'hyperémie réactive à l'aide de radiotraceurs. Dans cette étude, le nouvel outil de mesure est comparé à la pléthysmographie par jauge de contrainte (strain gauge). La méthodologie utilisée permet l'utilisation des deux systèmes de mesures d'une façon parfaitement simultanée. L'étude porte sur une cohorte de sujets non-sélectionnée. Nous exposons la nouvelle technologie et validons sa précision de mesure pour une large gamme de magnitude de flots artériels mesurés.

Le second article porte sur la mesure de la reproductibilité temporelle des mesures portant sur l'hyperémie réactive. De plus, nous tentons de caractériser la courbe hyperémique de façon à mieux identifier la portion endothéliale-dépendante. Ce manuscrit porte sur une population de sujets sains. Finalement, nous validons l'utilisation de la spectroscopie par infrarouge dans la quantification des phénomènes vasculaires présents dans la portion post-ischémique de l'hyperémie réactive.

Le troisième article traite de l'utilisation de la ventriculographie isotopique tomographique dans l'évaluation de la fonction ventriculaire gauche. Cette étude portant sur plus de 200 patients permet d'effectuer une validation de notre logiciel de segmentation ayant

récemment obtenu une protection par brevet pour le marché américain. La quantification de la fraction d'éjection du ventricule gauche est validée par comparaison avec la ventriculographie isotopique planaire. Nous effectuons également une comparaison directe avec un logiciel compétiteur (QBS, Cedar-Sinaï, CA).

Le dernier manuscrit expose les résultats de nos travaux portant sur la mesure de l'asynchronisme de contraction ventriculaire. Cette étude portant sur 235 patients démontre la méthodologie de mesure du CHI (Contraction Homogeneity Index), un nouvel indice permettant de quantifier d'une façon simple et précise, l'asynchronisme ventriculaire. Une analyse comparative est effectuée en utilisant l'écart type de la phase ventriculaire, calculée à l'aide de la ventriculographie planaire.

Contributions de l'auteur

Comme premier auteur du manuscrit intitulé, '*Mobil detection system to evaluate reactive hyperemia using radionuclide plethysmography*', nous avons conçu l'étude, écrit le protocole, participé au recrutement des patients, effectué les analyses des données, révisé la littérature, écrit le manuscrit, répondu aux commentaires de l'éditeur et soumis la version finale du texte. Les auteurs seniors, Jocelyn Dupuis et Paul Khairy ont contribué au contenu intellectuel des discussions, et ont révisé la première version et la version finale du manuscrit. Quam Ngo a contribué à l'ingénierie du prototype de mesure et à la réalisation des expériences. Vincent Finnerty a contribué à la création de la base de données. Edgar Hernandez (fellow étranger en cardiologie), a contribué au recrutement des sujets.

Dans le deuxième manuscrit intitulé, 'Arterial flow measurements during reactive hyperemia using NIRS', nous avons conçu l'étude et écrit le protocole, participé au recrutement des patients et effectué les analyses des données, révisé la littérature et écrit le manuscrit, répondu aux commentaires de l'éditeur et soumis la version finale du texte. Mme Nina Olamaei a effectué les expériences sur la cohorte de sujets et modélisé la réaction hyperémique. Jocelyn Dupuis a participé aux discussions intellectuelles et Paul Khairy a révisé les différentes versions du manuscrit en plus d'apporter son aide pour l'aspect statistique de l'étude.

Comme premier auteur du manuscrit intitulé, '*SPECT versus planar gated blood pool imaging for left ventricular evaluation*', nous avons conçu l'étude et effectué une recherche extensive de la littérature portant sur ce sujet. Nous avons effectué les analyse statistiques des données et rédigé l'ensemble des versions du manuscrit. Vincent Finnerty a participé activement à l'élaboration de l'algorithme de segmentation, assisté de Quam Ngo. Jean Grégoire et Bernard Thibault ont contribué aux contenus intellectuels des discussions tant en cardiologie nucléaire qu'en électrophysiologie cardiaque. Dr Paul Khairy a révisé la méthodologie et le manuscrit final.

Dans le dernier manuscrit intitulé, '*Comparison of left ventricular contraction homogeneity index using SPECT gated blood pool imaging and planar phase analysis*', nous avons conçu l'étude, analysé les données et écrit toutes les versions du manuscrit. Vincent Finnerty a participé à la collecte de l'ensemble des données provenant de la cohorte de patients inclus dans l'étude. Jean Grégoire et Bernard Thibault ont aidé au recrutement et à la réalisation des expériences effectuées au département de médecine nucléaire de l'Institut de Cardiologie de Montréal. Finalement, le Dr Paul Khairy a apporté son aide à l'analyse statistique en plus de réviser le manuscrit.

Manuscrits proposés

1. Mobile detection system to evaluate reactive hyperemia using radionuclide plethysmography (Physiol Meas. 2007 Aug;28(8):953-62.)

2. Arterial flow measurements during reactive hyperemia using NIRS (Physiol Meas. 2008 Sep;29(9):1033-40.)

3. SPECT versus planar gated blood pool imaging for left ventricular evaluation (J Nucl Cardiol 2007;14:544-9.)

4. Comparison of left ventricular contraction homogeneity index using SPECT gated blood pool imaging and planar phase analysis (J Nucl Cardiol. 2008 Jan-Feb;15(1):80-5.)

Mobile detection system to evaluate reactive hyperemia using radionuclide plethysmography

François Harel[1], Quam Ngo[1], Vincent Finnerty[1], Edgar Hernandez[1], Paul Khairy[2] and Jocelyn Dupuis[2]

1 Department of Nuclear Medicine, Montreal Heart Institute and Université de Montréal, Montreal, Quebec, Canada

2 Department of Medicine, Montreal Heart Institute and Université de Montréal, Montreal, Quebec, Canada

Received 20 March 2007, accepted for publication 11 June 2007 Published 30 July 2007
Online at stacks.iop.org/PM/28/953

Physiol. Meas. 28 (2007) 953–962
doi:10.1088/0967-3334/28/8/016

Abstract

We validated a novel mobile detection system to evaluate reactive hyperemia using the radionuclide plethysmography technique. Twenty-six subjects underwent simultaneously radionuclide plethysmography with strain gauge plethysmography. Strain gauge and radionuclide methods showed excellent reproducibility with intraclass correlation coefficients of 0.96 and 0.89 respectively. There was also a good correlation of flows between the two methods during reactive hyperemia *(r* = 0.87). We conclude that radionuclide plethysmography using this mobile detection system is a noninvasive alternative to assess forearm blood flow and its dynamic variations during reactive hyperemia.

Keywords: endothelium, radionuclide, reactive hyperemia

Venous plethysmography of the arms and legs has been extensively used to evaluate arterial inflow in normal and diseased states (Joyner *et al* 2001, Wilkinson and Webb 2001). This method allows evaluation of vascular reactivity during the local infusion of pharmacologic agents or reactive hyperemia. Although it has been well validated, the use of venous plethysmography to study arterial reactivity has been limited to research due to the need for specialized equipment and expertise not available in most clinical centers. As many studies indicate that the intensity of reactive hyperemia is modulated by the integrity of vascular endothelium (Farouque and Meredith 2003, Meredith *et al* 1996), several techniques were developed to measure hyperemic response after a brief ischemic period. Whereas strain gauge methods use circumferential measurements (Webb and Hand 1995, Hewlett and van Zwaluwenburg 1909) to derive arterial flow values, radionuclide plethysmography uses technetium-99m (^{99m}Tc) labeled autologous red-blood cell scintigraphy to measure radioactivity variations (which was also related to the arterial inflow during venous occlusion).

We recently validated the use of radioisotopes for measuring upper limb arterial blood flow with repeated venous occlusions (Harel *et al* 2005). This method uses autologous red blood cell labeling and a gamma-camera to detect variations of radioactivity in the arm. However, using a gamma-camera presents some drawbacks because the apparatus was not primarily designed to the image forearm blood flow. We therefore developed a novel device to measure forearm radioactivity variations. This device uses a clinical care recliner chair, onto which

two gamma-detector probes record radioactivity signals produced by labeled red blood cells included in both forearms. Venous occlusions produce an increase in limb volume distal to the occlusion site, with a rate of increase proportional to the arterial inflow. Repetitive occlusions therefore allow sequential arterial flow measurements during pharmacological intervention or reactive hyperemia.

The aim of this study was to compare forearm blood flow measurements using the gamma-detector probes with the well validated, strain gauge plethysmography during forearm reactive hyperemia (Roberts *et al* 1986).

Materials and methods

Patient population

Twenty-six subjects (23 men, 3 women) were recruited among patients scheduled for gated equilibrium radionuclide ventriculography scan at our nuclear medicine department. Mean age was 57 ± 14 years and body mass index was 26.8 ± 5.1 kg m^2. Patients had the following conditions: stable congestive heart failure *(n* = 13), stable angina *(n* = 13), prior myocardial revascularization with per-cutaneous coronary dilatation *(n* = 9) and/or coronary bypass *(n* = 6), diabetes *(n* = 4), high blood pressure *(n* = 15) and dyslipidemia *(n* = 15). Three were active smokers. The protocol was approved by our local research and ethics committees. All patients provided informed consent.

Venous plethysmography

Patients were seated in a recliner chair with arms prone and comfortably rested on the armrest. The chair was reclined so the forearms were above the level of the heart to prevent venous congestion. Venous cuffs were placed on the distal part of both arms and connected to an automatic pneumatic inflator (Hokanson, E-20 rapid cuff inflator; Bellevue, WA) set to 50 mmHg. Another cuff was placed proximally on the left arm and connected to a second pneumatic cuff inflator to provide arterial occlusion. For strain gauge plethysmography, calibrated mercury-in-silastic strain gauges were placed around both forearms 5 cm below the elbow crease and connected to the plethysmograph (Hokanson, model EC-4).

For radionuclide plethysmography, the gamma-detector probe (Ludlum, Sweetwater, TX, USA, model 44-2) was fixed under both armrests. The probe included a collimator (Ludlum, model 4002-227) and directed upward. Probe signals were linked to an electronic integrator (Ludlum, model 440-1) that generates a voltage proportional to the instantaneous count rate detected by each probe. Labeling of autologous red-blood cells was performed using the usual *in vivo* technique with intravenous administration of cold stannous pyrophosphate (Amerscan^{TM}, Amersham Health; Piscataway, NJ). We injected a dose (1100 MBq) of ^{99m}Tc 20 min later. This method provides labeling that is stable for many hours with excellent efficiency (>95%) (Saha 1998). Plethysmographic techniques were performed simultaneously. Data from the strain gauge plethysmograph and electronic integrator were digitized using a four-channel analog-to-digital converter (DI-148U,

DATAQ Instruments; Akron, OH). Radionuclide signals were normalized by individual baseline counts acquired before venous occlusion. This transformation provided compensation to variations in forearm volume and radionuclide dose injected and allowed inter-patient comparisons. Arterial inflow was calculated in the usual fashion by determining the upslope of the strain gauge and normalized radionuclide signals. Both techniques therefore provided relative flow changes.

Radionuclide data were transformed in two steps as previously detailed (Harel *et al* 2005). Briefly, we first corrected for inter-patient differences. These differences are related to variations in forearm volume and injected radionuclide dose. Inter-subject variations were corrected with normalization of each patient dataset using a baseline record. Baseline records quantify the amount of radioactivity in the opening window of the collimator, which is directly related to forearm volume and dose of radiotracer injected. In order to perform this correction, static acquisition of forearm radioactivity was obtained prior to the first venous occlusion and subsequent measurements were divided by this value.

A second correction involved calibration to convert radionuclide signals into flow units. We computed the mean of all post-hyperemic baseline-corrected data and mean of all strain gauge method data. The calibrating factor consisted of the ratio between these two means and was applied to post-hyperemic baseline-corrected data, providing data in the same units of measurement (ml/100 ml min^{-1}) as the strain gauge method.

Measurements protocol

Baseline flow measurements were performed with successive cycles of 10 s venous cuff occlusion and 10 s deflation cycles. Nine resting baseline flow measurements were made to assess reproducibility of both methods. After a 3 min resting period, rapid arterial occlusion of the left arm was provoked by inflating the arterial cuff for 5 min at 50 mmHg above the resting systolic pressure. The arterial cuff was then abruptly deflated and 21 cycles of venous compressions were performed. In order to increase the number of flow measurements in the post-ischemic period, venous compression and deflation cycles were decreased to 5 s for the first 2 min (12 cycles) followed by cycles of 10 s for the last 3 min of acquisition (9 cycles).

Statistical analysis

Statistical analysis was performed using the SPSS statistical package version 10.0 (SPSS; Chicago, IL). Reproducibility of baseline flow was assessed using intraclass correlation coefficients (ICC). Comparisons between the post-hyperemia arterial blood flow was assessed using repeated ANOVA and Bland–Altman analysis. Areas under curves (AUC) are expressed as mean ± SEM and compared with the Mann–Whitney test; all other values are expressed as mean ± SD. Statistical significance was accepted when the two-tailed p value was <0.05.

Results

During the baseline period, the venous occlusion applied to both arms created signal variations of the arm blood-pool compartment was clearly detected by radionuclide plethysmography (figure 1(A)) and the strain gauge method (figure 1(B)). The deflation period allowed enough time to reach the equilibrium of blood pool activity between the venous occlusion cycles.

Reproducibility

The strain gauge method showed excellent reproducibility with an ICC of 0.96 (95% CI: 0.95–0.98; $p < 0.0001$). The radionuclide method was likewise highly reproducible with an ICC of 0.89 (95% CI: 0.83–0.93; $p < 0.0001$), which was not different from the strain gauge approach.

Correlation of flow during reactive hyperemia

The effect of reactive hyperemia on forearm blood flow as a function of time is depicted for radionuclide and strain gauge methods in figure 2. Successive blood flow measurements, during reactive hyperemia with both methods were highly concordant (figure 3) with a correlation coefficient *(r)* of 0.87 (95% CI: 0.85–0.89; $p< 0.0001$). Comparisons between the two methods showed no statistically significant differences in post-hyperemia arterial blood flow at each time-point tested (overall $p= 1.0000$). Bland–Altman analysis is graphically depicted in figure 4. Systematic bias was negligible (0.000 02 ± 2.41 ml/ 100 ml min^{1}) and

linear regression of the bias versus mean value showed a slope not significantly different from zero (0.037 ± 0.022 ml/100 ml min^2; *p= 0.1)*.

Both methods were further compared by assessing the area under the flow–time curves (AUC) from deflation to 1 min of reactive hyperemia and from deflation to 5 min of reactive hyperemia. For the 1 min period, mean AUC was 8.48 ± 0.60 ml/ 100ml for the radionuclide method versus 8.44 ± 0.60 ml/ 100 ml for the strain gauge method. For the 5 min period, mean AUC was 20.90 ± 1.49 ml/ 100 ml for the radionuclide method and 20.93 ± 1.55 ml/ 100 ml for the strain gauge method. Mean AUCs were not statistically different between the two methods *(p* = 0.9).

Figure 5 shows the advantage of the radionuclide technique over the strain gauge plethysmography. Indeed, during an experience, the patient made a small tremor on one of his fingers, resulting in a marked artifact on the strain gauge signal. However, radionuclide signal remains mostly stable, allowing computation of the upslope of signal and accurate blood flow value.

Discussion

This study demonstrates that the use of a dedicated mobile system for radionuclide venous occlusion plethysmography can be used to non-invasively measure forearm blood flow and its dynamic variations during reactive hyperemia. This novel method provides excellent reproducibility and a good correlation with simultaneously performed strain gauge plethysmography, a method commonly used and recognized for the evaluation of endothelial

function and for vascular pharmacology studies (Farouque and Meredith 2003, Meredith *et al* 1996). The use of a dedicated mobile apparatus presents the advantage of allowing more flexibility in the choice of location for data acquisition.

Endothelial dysfunction is a diffuse process occurring early in the development of atherosclerotic vascular disease (Meredith *et al* 1993, Moncada and Higgs 1993). There is evidence that evaluation of endothelial function may be useful in risk stratification and in the evaluation of response to pharmacologic treatment (Leung *et al* 1993). In that context, development of a simple, non-invasive and reproducible test of the reactive hyperemic response is desirable not only for preclinical and clinical research purposes, but also for its potential clinical utility.

One additional advantage of our system is the automation of all acquisition procedures to reduce human intervention to a minimum. Indeed, venous and arterial cuffs were controlled by computer software. Therefore, the time of each occlusion was accurately programmed and remained the same for each patient. Moreover, data analysis including slope computation of the signal was also automatically made at the end of the study to provide immediate results without the need for offline analysis as is customary with strain gauge plethysmography. This automation process may reduce analysis bias and inter-patient variability.

Although both radionuclide and strain gauge approaches are based on the principle that variations in forearm volume during venous occlusion are proportional to arterial inflow, the measurement of forearm volume changes is obtained differently. Strain gauge plethysmography uses calibrated gauges that convert forearm perimeter variations to volume, while radionuclide plethysmography directly measures the activity of a blood pool tracer (labeled red blood cells) and assumes that it is proportional to blood volume. Small regional changes in the hematocrit do occur with higher blood flows and could affect the results (McHedlishvili *et al* 2003). Technically, measurement of the upslope of the variations in forearm volume with time is more difficult and subject to an experimental error at the higher flows. Although we subjectively found this limitation to be equally valid for both methods, it may significantly contribute to the greater variability with higher flows. We observed that one technical advantage of the radionuclide method is that it is less sensitive to patient's movements compared to the strain gauges that require absolute immobilization of the arms since any small movement can lead to a recorded artifact.

Meredith *et al* have previously studied reactive hyperemia with the use of strain gauge plethysmograph (Meredith *et al* 1996). They have also computed areas under the flow–time curves from deflation to 1 min and from deflation to 5 min and obtained measurements in good agreement with those reported in the present study. Others previously used vascular radioisotopes to quantify the hyperemic response. These studies however used a different approach and evaluated the first pass activity of vascular tracers after bolus injection. This

differs substantially from our methodology since we evaluated variations of the blood pool activity at equilibrium. Zicot *et al* injected ^{131}I-albumin to study first pass lower limb blood flow during reactive hyperemia in order to evaluate peripheral vascular disease of the legs (Zicot 1979). By comparison with strain gauge plethysmography, they found a good correlation between the time to peak of the isotopic activity curve and the width of the strain gauge hyperemic flow–time curve *(*$r = 0.74$; $p < 0.001$). In another study, Parkin *et al* studied patients who underwent brachial arteriotomy for coronary angiography. Using ^{99m}Tc-albumin and a first pass method associated during reactive hyperemia, they detected forearm ischemic complications of the brachial procedure (Moncada and Higgs 1993). The use of radionuclide with multiple occlusion technique was already studied in smaller population by other groups but they always used a gamma-camera to detect radioactivity variations (Clements *et al* 1981, Manyari *et al* 1988). More recently, Dupuis *et al* used ^{99m}Tc-tetrofosmin and compared the hyperemic response in a group of patients with demonstrated coronary artery disease and a group of subjects with no known coronary artery disease and no risk factors (Dupuis *et al* 2004). They compared the first pass activity of the hyperemic and non-hyperemic arms to derive parameters that were found predictive for the presence of coronary artery disease. These and the present study confirm the clinical potential of the use of radioisotopes for the dynamic evaluation of limb blood flow.

In comparison to the standard gamma-camera we have used in a previous study for radionuclide plethysmography, the mobile dedicated system provides better comfort for the

patient. Also, the results were more consistent between patients because both stimulus (reactive hyperemia) and measurements were under the automated control of software, which reduces procedural variations. Furthermore, since the amount of injected activity was the same as that used in a standard radionuclide ventriculography, this allows sequential procedures without supplementary puncture for the patient.

The fact that the radionuclide method uses a different detection mode compared to strain gauge plethysmography confers additional advantages. First, this method is less sensitive to movements that can occur during acquisition such as small movements of fingers accompanied by some contraction of the forearm muscle, which can be detected by the strain gauges. We have found that the isotopic method is less sensitive to these movement artifacts. Moreover, the use of a recliner chair optimizes the comfort and relaxation of the patient providing calm essential for this kind of experience. Also, in contrast to the gamma-camera, the recliner chair can be located anywhere in the hospital or clinic allowing the uses of small silent room that was impossible in a nuclear department (see figure 6). The patient irradiation was very low and due to the short half-life of radionuclide used, environmental load was negligible.

The mobile device was easy to build at an affordable cost. We used detector probes that were originally designed for thyroid uptake and adapted them to the recliner chair. The radiotracer utilized, ^{99m}technetium, is readily available in all nuclear medicine departments

and the radiation exposure for the patient and personal remains very low. However, the calibration factor used to convert the units obtained from the radionuclide method to flow units was specific to our experimental design and has to be re-validated if someone changes the detector or integrator used. The noise in the radionuclide system was higher than for the strain gauge system as seen in figure 1. However, slopes can be easily and automatically computed. We presently work on a new device with better radionuclide sensitivity.

We believe that this custom chair detection system represents a significant improvement compared to the gamma-camera that we have used in our previous study. This would allow more comfortable and faster procedures while assuring maximal reproducibility with software controlled procedures and analysis.

Conclusion

Radionuclide plethysmography is a new mobile system that allows serial measurements of arterial flow during reactive hyperemia. This novel, highly reproducible technique shows excellent concordance with the current gold standard, strain gauge plethysmography. From a practical perspective, this new tool may greatly increase accessibility to a rapid and accurate method of assessing vascular reactivity.

References

Clements I P, Strelow D A, Becker G P, Vlietstra R E and Brown M L 1981 Radionuclide evaluation of peripheral circulatory dynamics: new clinical application of blood pool scintigraphy for measuring limb venous volume, capacity, and blood flow *Am. Heart J.* 102 980–3

Dupuis J, Arsenault A, Meloche B, Harel F, Staniloae J and Gr´egoire J 2004 Quantitative hyperemic reactivity in opposed limbs during myocardial perfusion imaging a new marker of coronary artery disease JACC 2004

Farouque H M and Meredith I T 2003 Relative contribution of vasodilator prostanoids, NO and KATP channels to human forearm metabolic vasodilation *Am. J. Physiol. Heart Circ. Physiol.* 284 H2405–11

Harel F, Dupuis J, Benelfassi A, Ruel N and Gregoire J 2005 Radionuclide plethysmography for noninvasive evaluation of peripheral arterial blood flow *Am. J. Physiol. Heart Circ. Physiol.* 289 H258–62

Hewlett A and van Zwaluwenburg J 1909 The rate of blood flow in the arm *Heart* 187–97

Joyner M J, Dietz N M and Shepherd J T 2001 From Belfast to Mayo and beyond: the use and future of plethysmography to study blood flow in human limbs *J. Appl. Physiol.* 912431–41

Leung W H, Lau C P and Wong C K 1993 Beneficial effect of cholesterol-lowering therapy on coronary endotheliumdependent relaxation in hypercholesterolaemic patients *Lancet* 341 1496–500

Manyari D E, Malkinson T J, Robinson V, Smith E R and Cooper K E 1988 Acute changes in forearm venous volume and tone using radionuclide plethysmography *Am. J. Physiol.* 255 H947–52

McHedlishvili G, Varazashvili M, Kumsishvili T and Lobjanidze I 2003 Regional hematocrit changes related to blood flow conditions in the arterial bed *Clin. Hemorheol. Microcirc.* 29 71–9

Meredith I T, Anderson T J, Uehata A, Yeung A C, Selwyn A P and Ganz P 1993 Role of endothelium in ischemic coronary syndromes *Am. J. Cardiol.* 72 27C–31C; discussion 31C-32C)

Meredith I T, Currie K E, Anderson T J, Roddy M A, Ganz P and Creager M A 1996 Postischemic vasodilation in human forearm is dependent on endothelium-derived nitric oxide *Am. J. Physiol.* 270 H1435–40

Moncada S and Higgs A 1993 The L-arginine-nitric oxide pathway *N. Engl. J. Med.* 329 2002–12

Roberts D H, Tsao Y and Breckenridge A M 1986 The reproducibility of limb blood flow measurements in human volunteers at rest and after exercise by using mercury-in-Silastic strain gauge plethysmography under standardized conditions *Clin. Sci. (Lond.)* 70 635–8

Saha G B 1998 *Fundamentals of Nuclear Pharmacy* 4th edn (New York: Springer)

Webb D and Hand M 1995 Assessment of the effects of drugs on the peripheral vasculature *Clinical Measurement in Drug Evaluation* ed Nimmo W and Tucker G(London: Wiley) pp 136–50

Wilkinson I B and Webb D J 2001 Venous occlusion plethysmography in cardiovascular research: methodology and clinical applications *Br. J. Clin. Pharmacol.* 52 631–46

Zicot M 1979 Comparison of an isotopical and a plethysmographic method of assessing the distal blood flow during a reactive hyperemia in the lower limbs *Vasa* 8 102–8

Figures

Figure 1. Baseline measurements from (A) radionuclide plethysmography and (B) strain gauge plethysmography.

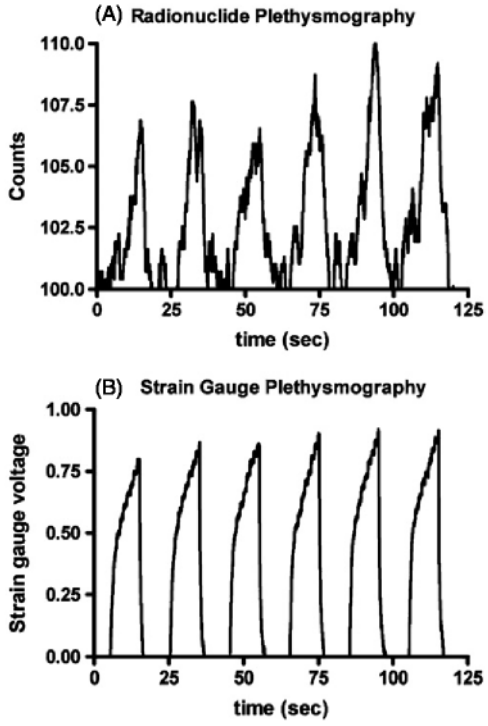

Figure 2. Typical example of strain gauge and radionuclide plethysmography forearm blood flow during reactive hyperemia by strain gauge (ml/100 ml min^{-1}) and radionuclide methods (ml/ 100 ml min^{-1}). The hyperemia starts after 3 min of baseline recording and 5 min of ischemia. Error bars represent SEM.

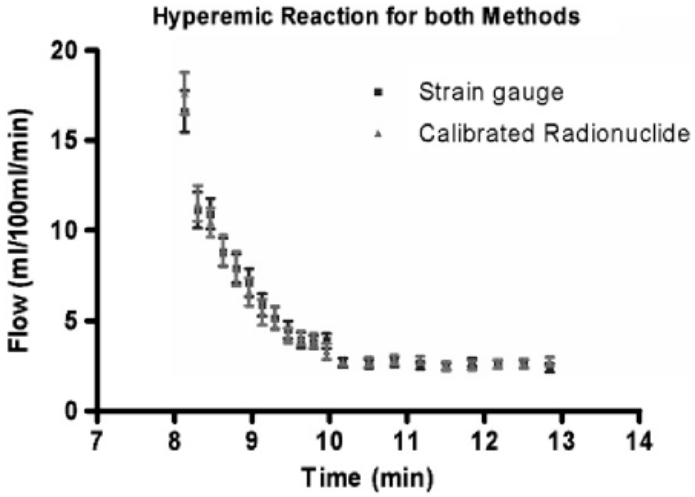

.

Figure 3. Post-hyperemic relational graph.

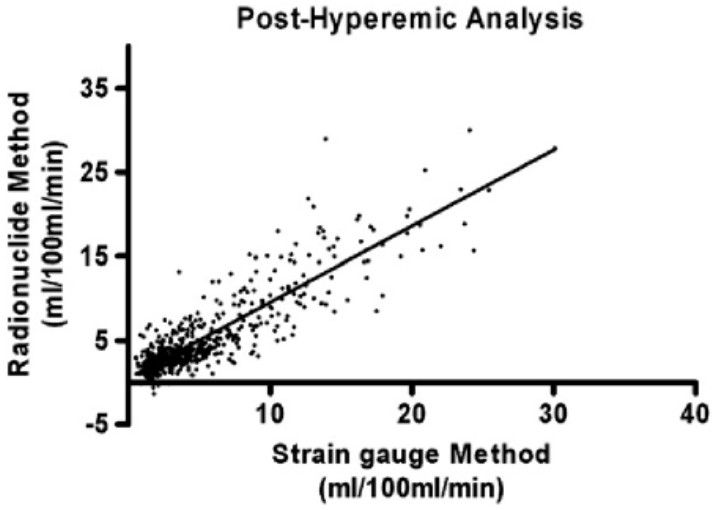

Figure 4. Bland–Altman graph of post-hyperemic flow.

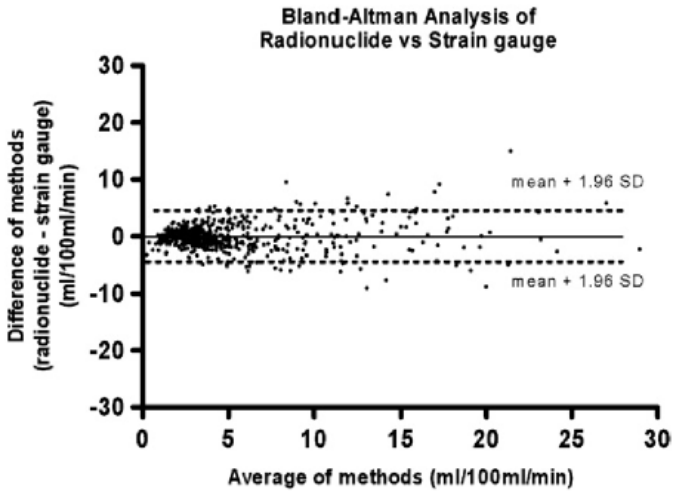

Figure 5. Example of movement artifacts detected by strain gauge and radionuclide plethysmography and created by discrete movements of the patient finger. Radionuclide signal (A) remains stable, allowing the computation of the arterial flow at this particular time. However, strain gauge signal was highly contaminated (B) making impossible calculation of the upslope and therefore arterial inflow.

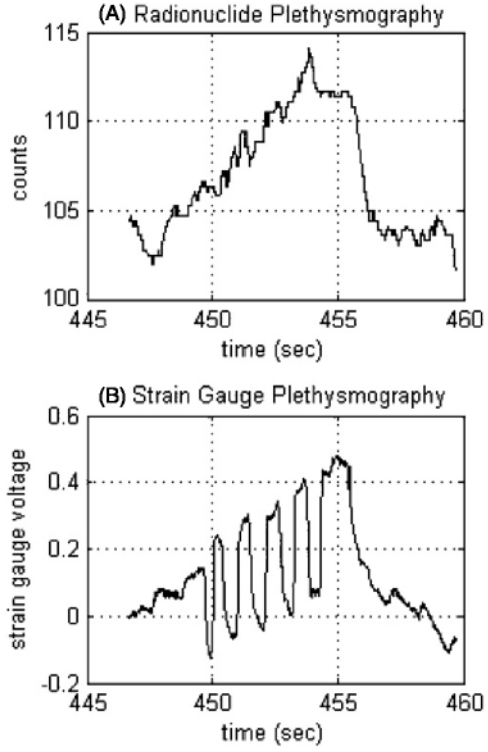

Figure 6. (A) The mobile recliner chair allowing easy and simple detection procedure with close-up on the radioactivity probe fixed under the armrest (B).
(This figure is in color only in the electronic version)

Arterial flow measurements during reactive hyperemia using NIRS

François Harel[1], Nina Olamaei[1], Quam Ngo[1], Jocelyn Dupuis[2] and Paul Khairy[2]

1 Department of Nuclear Medicine of the Montreal Heart Institute, Montreal, Quebec, Canada

2 Department of Medicine of the Montreal Heart Institute, Montreal, Quebec, Canada

Received 26 March 2008, accepted for publication 8 July 2008 Published 13 August 2008

Online at stacks.iop.org/PM/29/1033

Physiol. Meas. **29** (2008)1033–1040 doi:10.1088/0967-3334/29/9/003

Abstract

Non-invasive evaluation of peripheral perfusion may be useful in many contexts including clinical research. We validated a novel non-invasive spectroscopy technique to quantify forearm arterial inflow. This method, which is based on the measurement of tissular total hemoglobin variations after an ischemic period, was compared to strain gauge plethysmography (SGP). The technique uses near-infrared spectroscopy (NIRS) to determine the rate of change of forearm tissue oxygenation during reactive hyperemia. In this study, 13 subjects were simultaneously evaluated with NIRS and SGP. Nine baseline flow measurements were performed to assess the reproducibility of each method. Twenty-seven serial measurements were then made to evaluate flow variation during forearm reactive hyperemia. SGP and NIRS methods showed excellent reproducibility with the same intra-class correlation coefficients (0.98). In conclusion, the NIRS technique appears well suited for non-invasive evaluation of quantitative arterial forearm flow.

Keywords: NIRS, arterial flow, reactive hyperemia

Introduction

Atherosclerosis is a very prevalent disease. The coronary effects of this illness are a major cause of death and morbidity. Endothelial dysfunction is a systemic pathology, which is reversible and was considered to be the precursor that triggered coronary atherosclerosis (Behrendt and Ganz 2002, Weiss *et al* 2002). This condition can be assessed in a catheterization laboratory by coronary injection of acetylcholine that stimulates the release of endogenous NO (Forstermann *et al* 1988, Ludmer *et al* 1986, Werns *et al* 1989). Beside this invasive methodology, several authors studied various less invasive methods testing the peripheral endothelial function, which seems to correlate in a narrow way to coronary function endothelial activity (Anderson *et al* 1995). Strain gauge plethysmography (SGP) was used in association with vaso-active agonists and antagonists to assay the endothelial function in limbs (Creager *et al* 1992, Gerhard *et al* 1996). However, this technique requires arterial catheterization for peptide injection. Reactive hyperemia makes it possible to stimulate the peripheral endothelial function in a less invasive way. The technique was based on the creation of a temporary ischemic condition by an arterial compression that markedly decreases the vascular impedance distal to the occlusion site. The transition state at the release of ischemia generates the shearing forces, which stimulate the endogenous secretion of NO. The endogenous NO is a vasodilation agent causing the increase of arterial inflow. Thus this methodology indirectly measures the quantity of endogenous NO that was located in the vascular endothelium. Many techniques were used to detect the hyperemic reaction. SGP was used with repeated venous occlusion, providing sequential arterial

inflow measurements during hyperemia (Meredith *et al* 1996). We previously developed an isotopic technique that highly correlated with the SGP technique while being less sensitive to artifacts caused by patient movements (Harel *et al* 2005, 2008). In order to simplify the instrumentation, we used a near-infrared spectroscopy device trying to understand the relations between tissular oxygenation and arterial inflow (Harel *et al* 2008). However, the oximeter was originally intended to measure the cerebral oxygenation state and only provides the oxygenation index. Moreover, the device provides a too low sampling rate that could not accurately record all physiological variations during hyperemia. The goal of this study was to test the ability to accurately measure the forearm arterial flow during reactive hyperemia using a new near-infrared spectroscopy device. This new device outputs a higher sampling rate (6 Hz). It provides also several parameters such as variations in oxy-hemoglobin (ΔO_2Hb), deoxy-hemoglobin (ΔHHb) and total hemoglobin ($\Delta totHb$). We are interested in comparing the $\Delta totHb$ signal to the SGP signal, which are very similar.

Materials and methods

Patient population

Following approval by the internal research and the Ethics Committees at our institution and provision of informed consent, 13 subjects were included. We recruited participants who were scheduled for reactive hyperemia measurements. The cohort was composed of patients with few or no coronary disease risk factors.

The SGP method

The patients were sat in a quiet room, with arms resting in a supine position on supports positioned above the level of the heart to prevent venous congestion and facilitate spontaneous venous return. Venous cuffs were connected to automatic pneumatic inflators (Hokanson, E-20 rapid cuff inflator; Bellevue, WA) set to 50 mmHg. For the SGP method, calibrated mercury-in-silastic strain gauges were placed around both forearms 5 cm below the elbow crease and connected to a plethysmograph (Hokanson, model EC-4).

The NIRS method

A tissue oximeter (NIRO-200, Hamamatsu Corporation, Cambridge, MA) was used for the NIRS technique. The sensors use three wavelengths — 775, 810 and 850 nm — emitted in a sequential fashion. Each sensor also contains two detectors located at a mean distance of 4 cm from the emitting source. As the mean photon path in tissue has a 'banana' shape, increasing the source–detector distance provides a deeper absorption reading in tissue. Thus, the two sensors use these characteristics to remove contamination by perfusion in superficial tissue layers and essentially provide deeper regional hemoglobin oxygen saturation. This *in vivo* technique is based on the transmission through human tissues of near-infrared spectrum photons that are mainly absorbed by oxygenated and deoxygenated hemoglobin, cytochrome and myoglobin. NIRS is based on the Beer–Lambert law, which relates optical absorption to the concentration of light-absorbing chromophores present in a measured volume of tissue (Cheatle *et al* 1991).

For our study, sensors were fixed on the anterior aspect of both forearms, equidistant from the elbows, adjacent to the strain gauge and in a longitudinal orientation. These sensors contained an auto-adhesive surface that firmly sticks to the patient's skin, preventing displacement during measurements. The sensors were connected to the monitoring device via standard preamplifiers provided by the Hamamatsu Company. This oximeter provides several oxygenation parameters at a sampling rate of 6 Hz. These oxygen status values expressed the changes in total, oxygenated and deoxygenated hemoglobin and these signals were recorded, along with time base and other control codes, on a compatible personal computer using a custom acquisition program designed with MATLAB software. Curves of parameters were plotted in real time. In order to accurately compare both techniques, total hemoglobin signal (totHb) upslope, which represents forearm volume variations, was transformed using a unique calibration factor for all patients. This factor was computed with the same method as previously described to calibrate radionuclide signals (Harel *et al* 2005).

Data acquisition

SGP and NIRS techniques were then performed simultaneously. Data from the SGP were digitized using a four-channel analog-to-digital converter (DI-154 RS, DATAQ Instruments; Akron, OH). For the SGP method, arterial inflow was calculated in the usual fashion by determining the upslope of strain gauge signals. After removing the first and last seconds of the inflation period (venous occluded state), upslopes were calculated using a

linear regression model. Arterial flow values were expressed in mL dL^{-1} min^{-1}. Tissue oxygenation was expressed in change in specific hemoglobin in μmol L^{-1}.

Measurement protocol

Baseline flow measurements were performed with successive 10 s occlusion and deflation cycles of the venous cuff. Nine resting basal flow measurements were thus made in the pre-ischemic period, allowing the calculation of repeatability with both methods. In order to simulate variations in limb perfusion, we used the technique of reactive hyperemia. A second cuff was placed proximally on the left arm and connected to another pneumatic cuff inflator to provide arterial occlusion. After 3 min of rest, the rapid arterial occlusion of the left arm was inflated for 5 min at 50 mmHg above the resting systolic pressure. The arterial cuff was then spontaneously deflated to simulate reperfusion and 27 cycles of venous compressions were performed. In order to increase the number of flow measurements in the post-ischemic period, we decreased the time of venous compression and deflation to cycles of 5 s for the first 2 min (12 cycles) followed by cycles of 10 s for the last 5 min of acquisition (15 cycles). Throughout this data acquisition, strain gauge signals were acquired at 75 Hz and tissue oxygenation measurements at 6 Hz. All data were recorded in the computer for online processing and display.

Statistical analysis

The sample size was selected to provide 85% power to detect a difference of 0.1 mL · dL^{-1} · min^{-1} in forearm blood flow between SGP and NIRS, with a two-tailed alpha of 0.05. Normally distributed continuous variables are summarized by mean ± standard deviation (SD) unless specified. The reproducibility of baseline flow measurements with the SGP method and the NIRS signals was assessed using intraclass correlation coefficients (ICC) and compared with ANOVA tests. Comparison in peak flow was performed by a Wilcoxon matched pairs test. The normality of data distribution was assessed by Kolmogorov–Smirnov tests. Statistical significance was defined as a two-tailed *P*-value < 0.05. Statistical analysis was performed using the SPSS version 10.0 (SPSS; Chicago, IL) and Graphpad version 5.01 (GraphPad Software, San Diego, CA).

Results

Baseline characteristics

The mean age was 40 ± 14 years and 38% of the subjects were male. The body mass index was 28.2 ± 3.8 kg m^{-2}. The following medical conditions were present: stable congestive heart failure *(n* = 1), percutaneous coronary dilatation *(n* = 1), diabetes *(n* = 0), high blood pressure *(n* = 1) and dyslipemia *(n* = 2). Two patients were active smokers.

Baseline flow measurements

Nine measurements of baseline blood flow were taken for each upper limb. For the left arm, the baseline blood-flow was 3.36 ± 1.35 mL dL^{-1} min^{-1} with the SGP and 3.90 ± 1.74

mL · dL^{-1} · min^{-1} with the NIRS method *(p* = 0.10). These baselines values were used to test the reproducibility. The ICC were 0.98 (95% CI: 0.96–0.99; *P*< 0.0001) and 0.98 (95% CI: 0.95–0.99; *P*< 0.0001) for the SGP and NIRS methods, respectively. Both ICC expressed the same repeatability *(p* = NS).

Reactive hyperemia

During the ischemic period, we observed that the arterial inflows decrease with both methods. At the reperfusion state, we observed the flow restoration related to the hyperemic reaction. (figure 1). When we analyzed all flow measurements from all patients, the correlation coefficient between calibrated NIRS and SGP was 0.91 (figure 2). A Bland–Altman graph allowed better comparison between both methods. As shown in figure 3, NIRS tends to underestimate the high arterial inflows. Indeed, when we performed linear regression on the bias between both methodologies, the slope was evaluated to be -0.13 ± 0.019 and was significantly different from 0 ($p < 0.0001$). However, the goodness of fit for this regression was poor *(r* = 0.29).

Peak values during the reperfusion phase were evaluated to be 19.03 ± 5.65 mL dL^{-1} min^{-1} for SGP and 16.41 ± 3.63 mL · dL^{-1} · min^{-1} for NIRS. Peak values obtained by both techniques are significantly different *(p* = 0.048). These peak values corresponded to a *relative* augmentation of 566% and 421% for the SGP and NIRS techniques, respectively, compared to baseline values at rest.

We computed postline flow values with the last nine flow measurements of the experiment (the last 3 min of the experiment). These flows were located at the end of the reperfusion phase. Postline mean flows were evaluated at 2.70 ± 1.00 mL dL^{-1} min^{-1} for the SGP and 2.86 ± 0.93 mL $\cdot dL^{-1} \cdot min^{-1}$ for the NIRS method. These mean postline flows were significantly lower compared to their respective baseline values *(*p = 0.0005 for SGP and p = 0.0012 for NIRS).

Discussion

In the previous study, we have demonstrated that tissue oxygenation measurements could provide information reflecting the perfusion state of the measured limb, with potentially important clinical applications (*Harel et al 2008*). Unfortunately, the previous NIRS device was limited by a poor sampling rate of reading. Moreover, it provided a tissue oxygenation index, which was a composite parameter that reflects tissular oxygenation but cannot be used to generate arterial inflow values. In a repetitive venous occlusion setup, we need an evaluation of forearm volume in order to calculate the arterial inflows, this parameter being related to the upslope of the signal during the venous occlusion. Radionuclide plethysmography (RPG) was already developed in this way, providing another way to measure the volume variations with activity measurements of the forearm after red blood cell radiolabelling (Harel *et al* 2005, 2007). It had been shown that the RPG technique is well correlated with the SGP technique. However, the need for radionuclide injection as well as venous puncture can be limiting factors to a wide spread utilization. The

Niro-200 tissular oximeter provides many characteristics that can be useful to be included in an arterial inflow measurement setup. First, it provides a total hemoglobin variation parameter that was theoretically proportional to the volume of the analyzed region. Second, it generates up to six values per second, which offers enough reading points to accurately compute the upslope of the signal during the venous occlusion. These two characteristics allow the creation of a reactive hyperemic measurement system without any venous puncture, which may be used for widespread application of this technology.

In this study, the correlation between both modalities was good. However, in the Bland–Altman graph (figure 3), errors were higher at high flow values. These high flows occurred at the beginning of the reperfusion phase. At this moment, we chose to accelerate the flow measurement using a shorter venous occlusion period (5 s) instead of 10 s during the baseline part. This choice allowed better evaluation of this period where high variation of flow occurred. However, this occlusion period cannot be shorter in order to avoid volume accumulation in the forearm. Moreover, a shorter venous occlusion time decreases the number of recorded points, probably leading to less accurate results of the upslope computation. This can possibly explain the difference in the evaluation of the peak flows.

Baseline arterial inflow measurements obtained by both methods were very similar to those previously reported by Meredith *et al* (1996). However, we observed that after hyperemia postline flows were lower than their associated baseline values. Hyperemia seems to be responsible for this decrease. As basal flows were conditioned by many vasodilatator and

vasoconstrictor substances, this equilibrium seems to be unbalanced by hyperemia. In our setup, the duration of the experiment did not allow us to observe the recuperation of the flow to a value equal to the baseline. The non-zero arterial flow measured during the ischemic period was probably due to the periodic redistribution of the blood confined in the ischemic forearm caused by the venous occlusion.

Few studies related to forearm blood flow measurement using NIRS have been reported. These studies evaluate the performance of the NIRS method to measure blood flow by comparing it with different methods such as SGP and blood content analysis (De Blasi *et al* 1994, Edwards *et al* 1993, Van Beekvelt *et al* 2001). In our study, we simulate reactive hyperemia based on the literature to observe the physiological effect and we compare our observation with the SGP method, which is the gold standard (Pyke and Tschakovsky 2005). NIRS (NIRO2X-2, Keele University, UK) was already used by Jarm *et al* with a reactive hyperemia stimulus to study patients with peripheral vascular disease (Jarm *et al* 2003). They compared the NIRS method to laser Doppler flowmetry and transcutaneous oximetry. NIRS and Doppler flowmetry distinguished between healthy volunteers and patients with peripheral vascular disease (PVD). However, their methodology did not include venous compression, so NIRS did not provide measurements of arterial inflow. In our experiment, we can compare the flow values before and after reactive hyperemia.

Standardization of this technique is, however, required before widespread clinical application since variations in transducer location modify the signal response. In addition, in the near-infrared region, the myoglobin absorption spectrum overlaps that of hemoglobin (De Blasi *et al* 1991), but it is not relevant for this NIRS application because we measured the variation of total hemoglobin changes. In our setup design, the use of computer-based software allowed standardizing the methodology. Automated cuff inflation and signal interpretation likely contributed to increasing the repeatability and accuracy of the procedure.

Although the response of NIRS to ischemia and hyperemic reperfusion is generally similar in pattern to SGP, it remains unknown whether or not it measures the same regions of flow or same physiological responses as SGP and RPG. However, the similarity of the signals was obvious and we obtain a good correlation coefficient between both methods and this for a large variation of arterial inflow.

Conclusion

Accurate measurement of forearm arterial flow during reactive hyperemia is feasible in a totally non-invasive way using NIRS. This novel method has excellent reproducibility and can be used as a replacement for well-established SGP techniques.

Acknowledgment

This study was supported by the Fonds de la recherche en santé du Québec (FRSQ).

References

Anderson T J *et al* 1995 Close relation of endothelial function in the human coronary and peripheral circulations *J. Am. Coll. Cardiol.* **26** 1235–41

Behrendt D and Ganz P 2002 Endothelial function. From vascular biology to clinical applications *Am. J. Cardiol.* **90** 40L–48L

Cheatle T R, Potter L A, Cope M, Delpy D T, Coleridge Smith P D and Scurr J H 1991 Near-infrared spectroscopy in peripheral vascular disease *Br. J. Surg.* **78** 405–8

Creager M A, Gallagher S J, Girerd X J, Coleman S M, Dzau V J and Cooke J P 1992 L-arginine improves endothelium-dependent vasodilation in hypercholesterolemic humans *J. Clin. Invest.* **90**1248–53

De Blasi R A, Alviggi I, Cope M, Elwell C and Ferrari M 1994 Noninvasive measurement of forearm oxygen consumption during exercise by near infrared spectroscopy *Adv. Exp. Med. Biol.* **345** 685–92

De Blasi R A, Quaglia E and Ferrari M 1991 Skeletal muscle oxygenation monitoring by near infrared spectroscopy *Biochem. Int.* **25** 241–8

Edwards A D *et al* 1993 Measurement of hemoglobin flow and blood flow by near-infrared spectroscopy *J. Appl. Physiol.* **75** 1884–9

Forstermann U, Mugge A, Alheid U, Haverich A and Frolich J C 1988 Selective attenuation of endothelium-mediated vasodilation in atherosclerotic human coronary arteries *Circ. Res.* **62** 185–90

Gerhard M, Roddy M A, Creager S J and Creager M A 1996 Aging progressively impairs endothelium-dependent vasodilation in forearm resistance vessels of humans *Hypertension* **27** 849–53

Harel F, Denault A, Ngo Q, Dupuis J and Khairy P 2008 Near-infrared spectroscopy to monitor peripheral blood flow perfusion *J. Clin. Monit. Comput.* **22** 37–43

Harel F, Dupuis J, Benelfassi A, Ruel N and Gregoire J 2005 Radionuclide plethysmography for noninvasive evaluation of peripheral arterial blood flow *Am. J. Physiol. Heart Circ. Physiol.* **289** H258–62

Harel F, Ngo Q, Finnerty V, Hernandez E, Khairy P and Dupuis J 2007 Mobile detection system to evaluate reactive hyperemia using radionuclide plethysmography *Physiol. Meas.* **28** 953–62

Jarm T *et al* 2003 Postocclusive reactive hyperemia in healthly volunteers and patients with peripheral vascular disease measured by three noninvasive methods *Oxygen Transport to Tissue XXIV* ed J Dunn and H M Swartz (Dordrecht: Kluwer)

Ludmer P L *et al* 1986 Paradoxical vasoconstriction induced by acetylcholine in atherosclerotic coronary arteries *N. Engl. J. Med.* **315** 1046–51

Meredith I T, Currie K E, Anderson T J, Roddy M A, Ganz P and Creager M A 1996 Postischemic vasodilation in human forearm is dependent on endothelium-derived nitric oxide *Am. J. Physiol.* **270** H1435–40

Pyke K E and Tschakovsky M E 2005 The relationship between shear stress and flow-mediated dilatation: implications for the assessment of endothelial function *J. Physiol.* **568** 357–69

Van Beekvelt M C, Colier W N, Wevers R A and Van Engelen B G 2001 Performance of near-infrared spectroscopy in measuring local O(2) consumption and blood flow in skeletal muscle *J. Appl. Physiol.* **90** 511–9

Weiss N, Keller C, Hoffmann U and Loscalzo J 2002 Endothelial dysfunction and atherothrombosis in mild hyperhomocysteinemia *Vasc. Med.* **7** 227–39

Werns S W, Walton J A, Hsia H H, Nabel E G, Sanz M L and Pitt B 1989 Evidence of endothelial dysfunction in angiographically normal coronary arteries of patients with coronary artery disease *Circulation* **79** 287–91

Figures

Figure 1. Forearm blood-flow measured during reactive hyperemia by SGP and NIRS methods. Baseline measures were made during the first 3 min, then arterial occlusion was performed for 5 min in the left arm. Sudden restoration of the flow leads to reactive hyperemia. Dashed lines represent the mean ± sem for each point.
(This figure is in color only in the electronic version)

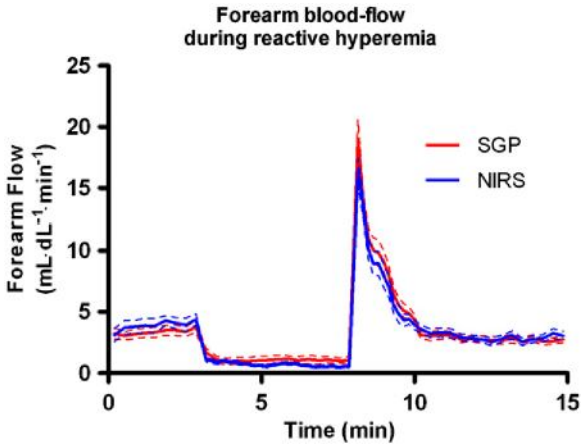

Figure 2. Relational graph allowing comparison between SGP and NIRS methodologies.

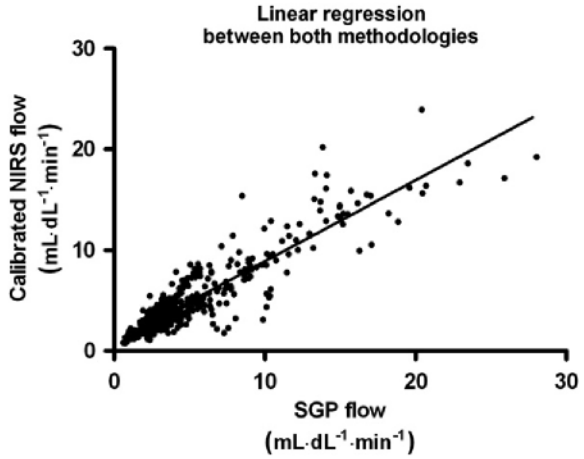

Figure 3. Bland–Altman graph of flow measurements.

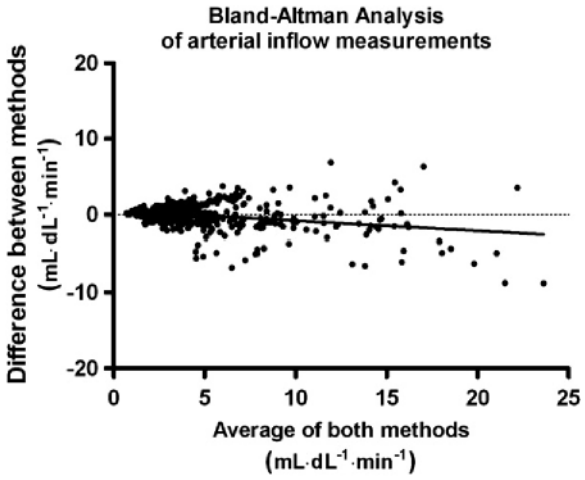

SPECT versus planar gated blood pool imaging for left ventricular evaluation

François Harel, MD,[a] Vincent Finnerty, MSc,[a] Quam Ngo, MSc,[a] Jean Grégoire, MD,[a] Paul Khairy, MD, PhD,[b] and Bernard Thibault, MD[b]

From the Departments of Nuclear Medicine, Montreal Heart Institute and Université de Montréal, Montreal, Quebec, Canada,[a] and Medicine, Montreal Heart Institute and

Université de Montréal, Montreal, Quebec, Canada[b].

Received for publication Oct 31, 2006; final revision accepted April 13, 2007.

Reprints request: François Harel, MD, Department of Nuclear Medicine, Montreal Heart Institute, 5000 Belanger St, Montreal, Quebec, H1T 1C8, Canada
1071-3581/$32.00

Doi:10.1016/j.nuclcard.2007.04.020

Résumé

Background. We developed a new segmentation algorithm based on the invariance of the Laplacian (IL) to compute volumes and ejection fractions and compared these results with planar analysis and gradients by use of a standard algorithm (QBS).

Methods and Results. Planar and single photon emission computed tomography blood pool acquisition was performed in 202 patients. Planar left ventricular ejection fraction (LVEF) was used as the gold standard, and single photon emission computed tomography images were processed by both 3-dimensional (3D) methods. Correlations between each 3D algorithm and planar methodology were as follows: r = 0.77 for QBS and r = 0.84 for IL. Mean LVEFs were 32.72% ± 13.05% for the planar method, 32.32% ± 15.98% for QBS, and 31.93% ± 13.44% for IL (P = .16). Bland-Altman analysis closely demonstrated negligible systematic bias for both 3D methods. Standard errors of bias were comparable between methods (9.36% for QBS and 7.44% for IL, P = .48). Linear regression of the Bland-Altman bias revealed a slope significantly different from 0 for the QBS method (0.22 ± 0.048, P<.0001) but not for IL (-0.032 ± 0.0044, P = .47).

Conclusion. The new segmentation algorithm provides comparable results to QBS and planar analysis. However, with QBS, the difference in LVEF was correlated with the magnitude of LVEF, which was not found with the new algorithm. (J Nucl Cardiol 2007;14:544-9.)

Key Words: Gated blood pool imaging • left ventricular ejection fraction

Gated cardiac blood pool imaging provides a simple and noninvasive method by which to assess ventricular function.[1-4] Planar equilibrium radionuclide angiography (ERNA) has long been considered the gold standard for left ventricular ejection fraction (LVEF), but the 2-dimensional projection images limit the accuracy of wall motion analysis related to blood structure overlap. Moreover, 2-dimensional images cannot analyze movements perpendicular to the detector, leading to multiple-view acquisition. Gated blood pool single photon emission computed tomography (GBPS), an extension to this technique, has been shown to improve the assessment of regional wall motion by removing the effects of chamber overlap.[5-9] However, despite a significant correlation with ERNA for LVEF computation, volume estimations of the left ventricle are less accurate. We developed segmentation software based on a new algorithm termed the invariance of the Laplacian (IL), used to analyze 3-dimensional (3D) blood pool images. This technique uses processing of multiple cutoff filters and finds a particular invariant point in the Laplacian of the filtered images. Our first results were compared with commercially available software (QBS, version 1.0; Cedars-Sinai Medical Center, Los Angeles, Calif) and planar estimates of LVEF.[10]

MATERIALS AND METHODS

Patient Population

The study population included 202 patients (45% male) referred for LVEF assessment between June 2004 and March 2005. Each patient underwent planar and tomographic blood pool acquisition. The mean age was 62 ± 12 years, and the mean body mass index was 27.6

± 5.1 kg/m^2. All patients had stable congestive heart failure based on the New York Association classification, and the following comorbidities were present: diabetes (n = 27), high blood pressure (n = 43), and dyslipidemia (n = 61). Nineteen patients were active smokers, and fifteen had a history of prior smoking. The protocol was approved by our local institutional review board.

Labeling technique

Labeling of autologous red blood cells was performed via the usual in vivo technique with intravenous administration of cold stannous pyrophosphate (Amerscan; Amersham Health, Piscataway, NJ) and 1110 MBq of technetium 99m 20 minutes later.

Planar acquisition

Planar equilibrium electrocardiography-gated radionuclide angiography was performed in all patients in the left anterior oblique projection, which optimized septal separation of the right ventricle and left ventricle. Clinical images were acquired on a planar single-head gamma camera (Scintronix, Livingston, England) with appropriate caudal tilt. A 20% energy window centered on 140 keV was used for acquisition, with a low-energy, high-resolution collimator. Images were acquired as 64 x 64 matrices at 5.33 mm per pixel. Gated acquisitions in 16 bins were performed with a 10% temporal window manually centered by use of a histogram of R-R intervals obtained before acquisition. The quality of planar images was controlled while ensuring a mean density count greater than 1000 counts per square centimeter per frame in the left ventricle on the optimal septal view.

Planar gated blood pool (GBP) images were transmitted to an Odyssey computer system (version FX 8.9C; Picker, Cleveland, Ohio), where processing was performed with commercially available software. For LVEF assessment, observers outlined the initial left ventricular (LV) contours at end systole and end diastole. They were guided by their visual impression of the LV shape aided by Fourier amplitude and phase maps. For all time intervals of the complete planar GBP study, algorithms generated regions automatically based on end-diastolic limits, which observers reviewed and modified as necessary. Background regions of interest (ROIs) were also drawn by use of a 2- to 3-pixel-wide crescent-shaped region positioned about 2 pixels away from the posterolateral wall.

GBPS data acquisition

Immediately after planar GBP image acquisition, all patients underwent GBPS. A triple-head gamma camera (Prism 3000S; Picker) was used to collect images at 63 projections over a 360° ellipsoidal arc. By use of a low-energy, high-resolution collimator, 64 x 64 tomograms with a pixel size of 5.32 mm were acquired for 45 accepted beats per projection. Tomograms were acquired at rest, with 16 frames per R-R interval and a 20% R-wave window. The quality of each acquisition was further controlled while ensuring a mean count density greater than 100 counts per square centimeter per frame in the left ventricle for the 3 raw projections with the ventricle in the optimal septal position.

All data sets were reviewed for any confounding imaging artifact. Ramp-filtering transaxial reconstructions were performed followed by 3D filtering with a Butterworth filter, order 5. Frequency cutoffs were selected with the aid of a power spectrum graph to remove frequencies where the signal-to-noise ratio was lower than 10%. Images were reoriented into short-axis sections by manual selection of approximate LV symmetry axes.

GBPS data processing

Data sets were processed by both QBS and IL algorithms. QBS, which was previously described by Van Kriekinge et al,[10] was a surface gradient method. The IL algorithm was based on the concept of the IL. Laplacian was defined as the sum of the second partial derivative in all dimensions. For a 1-dimensional figure (a simple curve), the Laplacian equals the curvature of the function. For a 3D surface, the Laplacian equals the rate of changing in all dimensions, which can be interpreted as a multidimensional slope or the curvature of the plane. Classical segmentation criteria such as the intensity threshold or the minimum of the derivative are considered accurate with unblurred images. However, with blurred images such GBPS images, these methods tend to retract inside sharp curves, thus underestimating convex volumes. Our algorithm was based on the computation of the Laplacian on the treated GBPS images with variable filters. The images were filtered with a variable cutoff frequency, and Laplacian was computed for each data set. We then found a pivotal point that was consistent for all filtered data sets, which represents the estimation of the true edge. Thus the found edges were invariant to the filter cutoff used (Figure 1). The

algorithm is divided into 3 parts: determination of initial surfaces, estimation of Laplacians, and determination of exact edge positions.

Initial surface. Watershed segmentation was first performed on the ungated image to isolate all structures of the 3D image.[11] The region corresponding to the left ventricle was determined by use of geometric assumptions (ie, the left ventricle should be near the center of the image and to the left of the right ventricle). A smoothed isosurface was then determined inside the left ventricle's region.

Estimation of Laplacians. The 3D Laplacian images were estimated via a frequency-based method. A modified Butterworth filter was used with multiple cutoff frequencies.

Exact edge position. Activity profiles were then estimated along directions perpendicular to the surface, allowing more precise samples than spherical coordinates or an initial ellipsoid. Each Laplacian image was sampled along 400 normal vectors to the isosurface, and we found a pivotal point, which minimized the variations of the Laplacian due to the filter cutoff. This same criterion was used for all ventricular walls including the mitral valve region.

Each LVEF computed by both 3D methods was compared with ERNA.

Statistical analysis

Statistical analyses were performed by use of GraphPad Prism software (version 4.03 for Windows; GraphPad Software, San Diego, Calif). Data are expressed as mean ± SD. Success rates in automated and manual modes were compared via Fisher exact tests. Ejection fractions calculated with planar and 3D methods were compared by use of the Friedman test or repeated-measures analysis of variance, where appropriate. Relationships between each 3D algorithm and planar methods were assessed by linear regression models. Error analyses of both 3D algorithms were performed by use of Bland-Altman graphs. Linear regression models were used to compare 3D algorithm errors.

RESULTS

Software region generation

QBS successfully automatically processed 180 (89%) of the 202 patients, and IL successfully automatically processed 188 (93%) *(P* = .22). With manual processing in the event of failed automated processing, QBS successfully processed 187 patients whereas IL processed 195 *(P* = .12). Finally, 182 patients were successfully processed by both algorithms, and this cohort was used for all further statistically analysis.

LVEF analysis

LVEFs with planar, QBS, and IL algorithms were 32.72% ± 13.05%, 32.32% ± 15.98%, and 31.93% ± 13.44%, respectively *(P* = .1603). Correlations were noted between LVEF computed by 3D methods and planar methods *(r* = 0.770 for QBS and *r* = 0.835 for IL). Linear regression of 3D methods compared with planar results revealed slopes near unity (with slopes of 0.99 ± 0.053 for QBS and 0.87 ± 0.041 for IL) (Figure 2); QBS was closer to the unity slope than IL *(P* = .002). Bland-Altman analysis of 3D versus planar methods indicated a systematic bias of -0.40% for QBS compared with -0.79% for IL. Standard errors of bias were comparable for QBS and IL (9.36% for QBS and 7.44% for IL, *P* = .48) (Figure 3). Linear regression of the Bland-Altman bias showed that for the QBS method, the slope was significantly different from 0 (0.22 ± 0.048; F = 22, *P* = .0001). For IL, the slope of -0.032 ± 0.0044 was not significantly different from 0 (F = 0.54, *P* = .47). When QBS was compared with IL, the correlation was 0.78 and the estimated bias was calculated to be 0.38% ± 10.0%.

Volume analysis

IL methodology provided end-diastolic and endsystolic ventricular volume estimates that correlated well with QBS algorithms. For end-diastolic volumes, the correlation was 0.895 and the linear regression slope was 0.80 ± 0.030 (Figure 4). The intercept of the linear regression curve was significantly different from 0 (*y* = 64 ± 7 mL, *P* = .0001). For end-systolic volumes, the correlation was 0.931, with a slope of 0.88 ± 0.026.

DISCUSSION

LVEF remains an important parameter for determining the prognosis of patients. Several methods allow this parameter to be assessed via several techniques and technologies. Despite the prominent role of echocardiography in current medical practice, ventriculography continues to be indicated when the degree of accuracy is an issue, such as during follow-up after chemotherapy. Isotopic ventriculography in tomographic mode is an extension of the planar method. Several algorithms were developed to allow measurement of various ventricular parameters.

Overall, we found no significant differences between the 2 tomographic algorithms for successful automation. The correlation for LVEF between 3D and planar methods is comparable to previously published results.[12,13] Successful automation generally decreases intraobserver variability by eliminating a human intervention. For both 3D algorithms, failure to compute LVEF was the result of segmentation problems related to poor statistic counting images, and most of these images were problematic for both 3D algorithms.

In general, the strength of a method lies in its estimate of LVEF rather than volumes. Error cancellation was probably the reason for these high correlation coefficients. LVEF is generally underestimated in planar mode, related to the persistent atrial activity in the systolic area of interest. We did not observe a significant difference between ejection fractions in planar and tomographic modes in our results.

The correlation between results obtained in planar and tomographic modes was comparable for both 3Dmethods. Analyses suggest that QBS tends to overestimate LVEF values whereas IL tends to underestimate them. QBS has a bias SD higher than IL, which is correlated with ejection fraction. QBS therefore becomes less precise with higher values of LVEF. IL has a more stable bias, not correlated with the value of the ejection fraction.

Groch et al [8,14,15] previously studied other algorithms for cardiac blood pool segmentation. They reported a significant correlation between their 3D method and planar ventriculography *(r* = 0.92), but unlike our study, their method generated a bias that correlated with the magnitude of the LVEF. Bartlett et al also studied cardiac blood pool segmentation using a retroprojected long-axis view.[9] They also found a correlation with planar methodology *(r* = 0.89), although the study was limited to a small population. More recently, Eder et al [16] used a real 3D segmentation technique that provided correlation with planar results *(r* = 0.90). In addition, Daou et al[17] compared a new segmentation algorithm with planar methodology and found a correlation for LVEF of 0.62. Although correlation with planar methodology is certainly a valuable endpoint, it is not an ideal gold standard. The planar method has its own limitations, such as the location of the background ROI or the inclusion of the ascending aorta in the LV ROI. More accurate methodology such as magnetic resonance imaging was used by Nichols et al [18] in a population with congenital disease. Analysis of volume estimation was also limited by the fact that no independent

gold standard method was used to clearly estimate the true volume measurement. We are currently investigating comparisons with magnetic resonance imaging as a gold standard in normal patients and patients with heart failure.

Study limitations

All tomographic acquisitions were carried out for 360°, and thus our algorithm requires validation for 180° acquisition. Planar acquisitions were performed with only 16 bins, and as compared with acquisitions with 24 to 32 bins, LVEF may be underestimated. However, the same number of bins was used in both planar and single photon emission computed tomography acquisition, leading to a more direct comparison. Contrary to planar ventriculography, which is based on counts, the 2 tomographic methods are space-based. Unlike count-based algorithms, space-based algorithms do not capitalize on the independence of ventricular form. On the contrary, space-based methods capitalize on the weakness of isotopic imagery, the poor spatial resolution. These methods nevertheless appear reliable, robust, and useful. Moreover, tomographic ventriculography is a noninvasive technique and is much more widely available than magnetic resonance or multidetector computed tomography scans.

In conclusion, we propose a novel algorithm for the evaluation of LVEF that agrees with the planar LVEF values and appears reliable across the range of LVEFs tested. The

success rate for automated processing is high, decreasing the need for manual intervention. Further studies are required to validate volume calculation as well.

Acknowledgment

The authors have indicated they have no financial conflicts of interest.

References

1. Bacharach SL, Green MV, Borer JS. Instrumentation and data processing in cardiovascular nuclear medicine: evaluation of ventricular function. Semin Nucl Med 1979;9:257-74.
2. Bonaduce D, Morgano G, Petretta M, Arrichiello P, Conforti G, Betocchi S, et al. Diastolic function in acute myocardial infarction: a radionuclide study. J Nucl Med 1988;29:1786-9.
3. Bonow RO, Bacharach SL, Green MV, Kent KM, Rosing DR, Lipson LC, et al. Impaired left ventricular diastolic filling in patients with coronary artery disease: assessment with radionuclide angiography. Circulation 1981;64:315-23.
4. Strauss HW, Zaret BL, Hurley PJ, Natarajan TK, Pitt B. A scintiphotographic method for measuring left ventricular ejection fraction in man without cardiac catheterization. Am J Cardiol 1971;28:575-80.
5. Corbett JR, Jansen DE, Lewis SE, Gabliani GI, Nicod P, Filipchuk NG, et al. Tomographic gated blood pool radionuclide ventriculography: analysis of wall motion and left ventricular volumes in patients with coronary artery disease. J Am Coll Cardiol 1985;6:349-58.
6. Fischman AJ, Moore RH, Gill JB, Strauss HW. Gated blood pool tomography: a technology whose time has come. Semin Nucl Med 1989;19:13-21.

7. Gill JB, Moore RH, Tamaki N, Miller DD, Barlai-Kovach M, Yasuda T, et al. Multigated blood-pool tomography: new method for the assessment of left ventricular function. J Nucl Med 1986;27:1916-24.

8. Groch MW, Marshall RC, Erwin WD, Schippers DJ, Barnett CA, Leidholdt EM Jr. Quantitative gated blood pool SPECT for the assessment of coronary artery disease at rest. J Nucl Cardiol 1998;5:567-73.

9. Bartlett ML, Srinivasan G, Barker WC, Kitsiou MN, Dilsizian V, Bacharach SL. Left ventricular ejection fraction: Comparison of results from planar and SPECT gated blood-pool studies. J Nucl Med 1996;37:1795-9.

10. Van Kriekinge SD, Berman DS, Germano G. Automatic quantification of left ventricular ejection fraction from gated blood pool SPECT. J Nucl Cardiol 1999;6:498-506.

11. Vincent L, Soille P. Watersheds in digital spaces: an efficient algorithm based on immersion simulations. IEEE Trans Pattern Anal Mach Intell 1991;13:583-98.

12. De Bondt P, De Winter O, De Sutter J, Dierckx RA. Agreement between four available algorithms to evaluate global systolic left and right ventricular function from tomographic radionuclide ventriculography and comparison with planar imaging. Nucl Med Commun 2005;26:351-9.

13. Odagiri K, Wakabayashi Y, Tawarahara K, Kurata C, Urushida T, Katoh H, et al. Evaluation of right and left ventricular function by quantitative blood-pool SPECT

(QBS): comparison with conventional methods and quantitative gated SPECT (QGS). Ann Nucl Med 2006;20:519-26.

14. Groch MW, DePuey EG, Belzberg AC, Erwin WD, Kamran M, Barnett CA, et al. Planar imaging versus gated blood-pool SPECT for the assessment of ventricular performance: a multicenter study. J Nucl Med 2001;42:1773-9.

15. Groch MW, Schippers DJ, Marshall RC, Groch PJ, Erwin WD. Quantitative gated blood pool SPECT: analysis of 3-dimensional models for the assessment of regional myocardial wall motion. J Nucl Cardiol 2002;9:271-84.

16. Eder V, Bernis F, Drumm M, Diarra MI, Baulieu F, Leger C. Three-dimensional analysis of left ventricle regional wall motion by using gated blood pool tomography. Nucl Med Commun 2004;25:971-8.

17. Daou D, Coaguila C, Benada A, Razzouk M, Haidar M, Colin P, et al. The value of a completely automatic ECG gated blood pool SPECT processing method for the estimation of global systolic left ventricular function. Nucl Med Commun 2004;25:271-6.

18. Nichols K, Saouaf R, Ababneh AA, Barst RJ, Rosenbaum MS, Groch MW, et al. Validation of SPECT equilibrium radionuclide angiographic right ventricular parameters by cardiac magnetic resonance imaging. J Nucl Cardiol 2002;9:153-60.

Figure 1. Graphic explanation of IL algorithm for edge detection of an arbitrary point. The *dashed line* represents the theoretic edge. The *solid line* represents this edge seen by a detection system such as a gamma camera. The *dotted lines* represent 3 Laplacian images with different blurring. The invariance point is shown by a *circle*

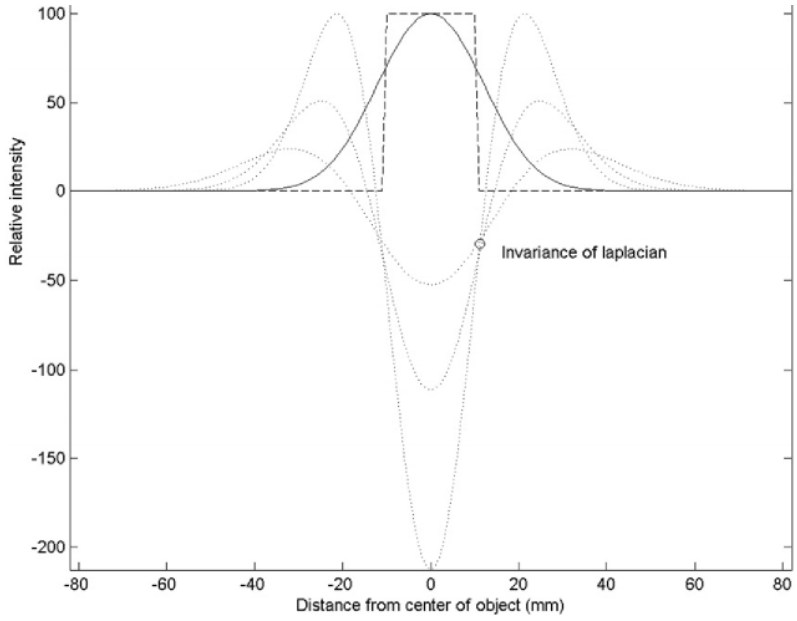

Figure 2. Regression analyses showing associations between 3D methods and planar method for LVEF computation for QBS **(A)** and IL **(B)** algorithms.

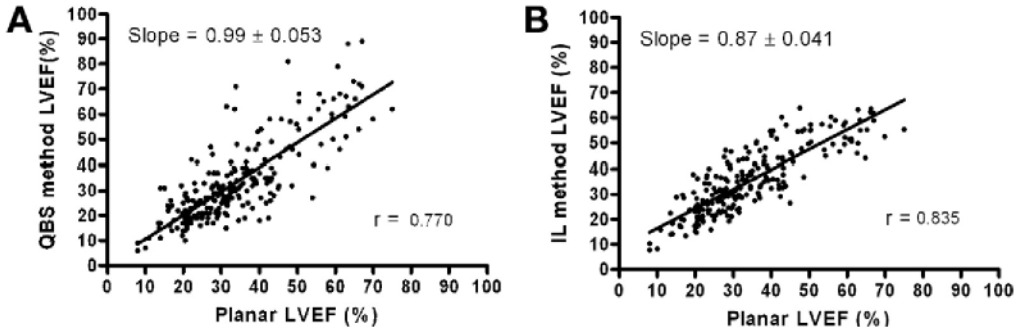

Figure 3. Bland-Altman graphs showing comparison of LVEF assessment by QBS **(A)** and IL **(B)** algorithms versus planar results. **C,** Direct comparison between both 3D algorithms.

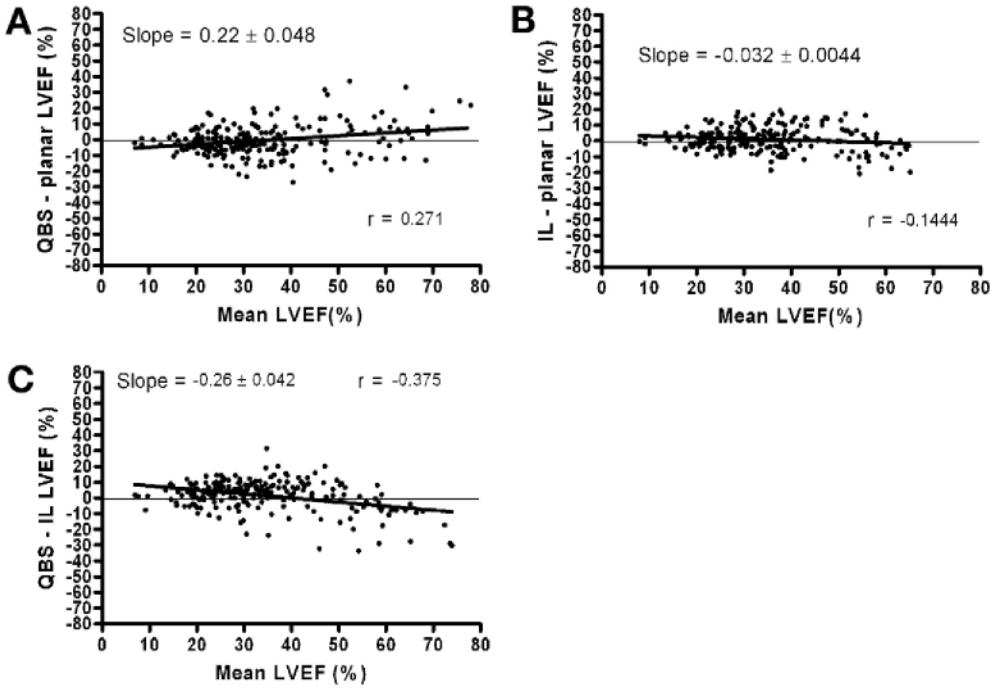

Figure 4. Comparison between IL and QBS algorithms for evaluation of end-diastolic volume *(EDV)* **(A)** and end-systolic volume *(ESV)* **(B).**

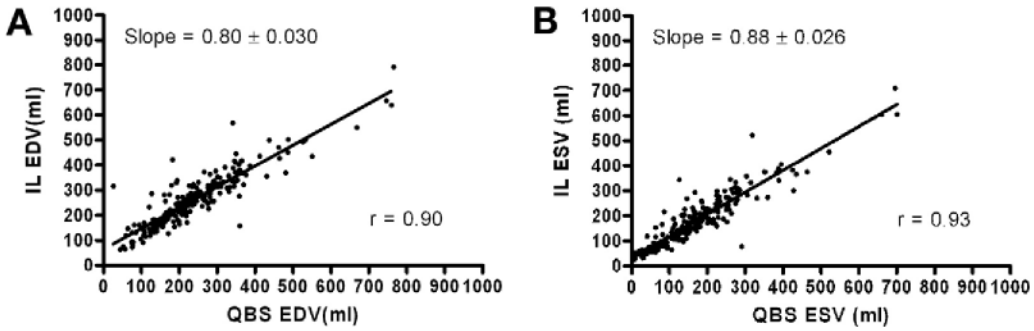

Comparison of left ventricular contraction homogeneity index using SPECT gated blood pool imaging and planar phase analysis

François Harel, MD, BEng,[a] Vincent Finnerty, MSc,[a] Jean Grégoire, MD,[a] Bernard Thibault, MD,[b] and Paul Khairy, MD, PhD[b]

Journal of Nuclear Cardiology; 2008 Jan-Feb;15(1):80-5.

From the Departments of Nuclear Medicine[a] and Medicine,[b] Montreal Heart Institute and Université de Montréal, Montreal, Quebec, Canada.

This work was supported in part by the "Fonds de la Recherche en Santé du Québec" and by a Canada Research Chair.

Received for publication April 30, 2007; final revision accepted July 26, 2007.

Reprint requests: François Harel, MD, BEng, Department of Nuclear Medicine,
Montreal Heart Institute, 5000 Belanger St, Montreal,
Quebec, H1T 1C8, Canada
1071-3581/$34.00

doi:10.1016/j.nuclcard.2007.07.015

Abstract

Background. There is growing interest in developing a practical technique to accurately assess ventricular synchrony. We describe a novel 3-dimensional (3D) gated blood pool single photon emission computed tomography (SPECT) approach, from which a contraction homogeneity index (CHI) is derived and compared with planar phase analyses.

Methods and Results. Subjects underwent planar and SPECT blood pool acquisition. Planar images were processed for left ventricular ejection fraction computation and phase values. SPECT images were processed by our novel algorithm, with which CHI was computed. Overall, 235 patients (79% male; mean age, 62 ± 11 years) completed the study. Left ventricular ejection fractions were similar by planar (33.5% ± 13.5%) and 3D (34.7% ± 12.7%) methods *(r* = 0.83, *P*<.0001). Mean phase angles for planar and tomographic methods were 126.3° ± 29.6° and 124.4° ± 28.7°, respectively *(r* = 0.53, *P*<.0001). Phase and amplitude signals were incorporated in the CHI, which was non-normally distributed with a median of 73.8% (interquartile range, 58.7%-84.9%). This index minimized the negative impact of dyskinetic wall segments with limited regional motion. The planar heterogeneity index (SDΦ) was 28.2° (interquartile range, 17.5°-46.8°) and correlated inversely with CHI *(r* = -0.61, *P*<.0001).

Conclusion. The novel 3D dispersion index CHI accounts for both phase delay of a dyssynchronous segment and its magnitude of contraction and is moderately correlated with planar phase analyses. Its potential in cardiac resynchronization therapy remains to be exploited. (J Nucl Cardiol 2008;15:80-5.)

Key Words: Contraction homogeneity index single photon emission computed tomography gated blood pool imaging cardiac resynchronization therapy

Congestive heart failure has been labeled an epidemic of modern times. Over the past 5 years, several large-scale clinical trials have demonstrated salutary effects of cardiac resynchronization therapy (CRT) in selected patient populations,[1-4] spawning an interest in refining techniques to assess ventricular dyssynchrony. These have encompassed various types of analyses via radionuclide ventriculography, including a dispersion index derived from planar phase imaging (SDΦ). Given the increasing interest in and recognized potential of gated blood pool (GBP) single photon emission computed tomography (SPECT), we sought to compare planar phase imaging with a novel ventricular contraction homogeneity index (CHI) derived from this technology.

MATERIALS AND METHODS

Study population

The study population consisted of consecutive patients referred to the Department of Nuclear Medicine at the Montreal Heart Institute (Montreal, Quebec, Canada) for assessment of left ventricular (LV) systolic function between June 2004 and June 2006. Patients hospitalized for an acute event or with decompensated heart failure were excluded. Data regarding baseline variables and past medical history were recorded, and both planar and GBP SPECT acquisitions were performed. The protocol was approved by the Montreal Heart Institute's research and ethics committees.

Labeling technique

Labeling of autologous red blood cells was performed by the usual in vivo technique with intravenous administration of 1110 MBq technetium 99m. Cold stannous pyrophosphate (Amerscan; Amersham Health, Piscataway, NJ) was injected 20 minutes before technetium administration.

Planar acquisition

Planar equilibrium electrocardiography-gated radionuclide angiography was performed in the left anterior oblique projection to optimize septal separation of the right ventricle from the left ventricle. Clinical images were acquired on a planar gamma camera (Scintronix, Livingston, England) with appropriate caudal tilt. A low-energy, high-resolution collimator was used for acquisition, with a 20% energy window centered on 140 keV. Images were acquired as 64 x 64 matrices at 5.33 mm/pixel, and acquisition was gated via a 20% temporal window manually centered by use of the R-R histogram and 16 bins. The quality of planar images was controlled while ensuring an LV count density greater than 500 counts/ cm^2 per frame on the best septal view.

Planar GBP images were processed with commercially available software (version FX 8.9C; Picker, Cleveland, Ohio). For assessment of LV ejection fraction (EF), an operator outlined LV contours at end systole and diastole, guided by a visual impression of LV shape and assisted by Fourier amplitude and phase maps. For all other time intervals in the

complete planar GBP study, automated algorithms generated regions based on end-diastolic and end-systolic limits. Mean phase angle and planar heterogeneity indices were computed, with the latter defined as the SD of the phase signal within the LV region. As the planar software uses a sine rather than cosine function to perform harmonic analyses, we factored in a 90° constant to all planar mean phases to compare 3-dimensional (3D) and planar methods.

GBP SPECT data acquisition

Immediately after planar GBP image acquisition, all patients underwent GBP SPECT. A triple-head gamma camera (Prism 3000S; Picker) was used to collect images in 63 projections over a 360° ellipsoidal arc. With a low-energy, high-resolution collimator, 64 x 64 tomograms with a pixel size of 5.32 mm were acquired per projection for 45 accepted cycles. Tomograms were acquired at rest, with 16 frames per R-R interval and a 20% R-wave window. The quality of each acquisition was further controlled while ensuring a count density greater than 100 counts/cm^2 per frame in the 3 projections with the left ventricle in the best septal position.

All data sets were reviewed for potential imaging artifacts. Ramp-filtering transaxial reconstructions were performed followed by 3D filtering with a Butterworth order-5 filter. Frequency cutoffs were selected with the aid of a power spectrum graph to remove all frequencies with a signal-to-noise ratio of less than 10%. Images were reoriented into short-

axis sections by manually selecting LV symmetry axes. Segmentation of short-axis slices was performed with in-house software by use of a technique based on invariance of the Laplacian.[5] For each vertex of the LV surface in motion, Fourier analysis gave 2 parameters: amplitude and phase (or delay) of contraction. A third parameter was derived from these values. Contraction efficiency (E) of a vertex is the portion of its contraction amplitude that is in phase with the remainder of the ventricle. E was computed in the Fourier space as the projection along the direction of the mean phase. Thus E is negative if the vertex phase differs from the mean phase for more than a quarter of the cardiac cycle. CHI constitutes a transformation of the ratio between wall movement contributing to stroke volume and total wall movement. CHI, therefore, relates the ratio of mean efficiency to mean amplitude.

$$CHI\ \alpha\ \frac{\overline{E}}{\overline{A}}$$

in which $\overline{E}$ is the mean efficiency and $\overline{A}$ is the mean amplitude of ventricular wall movements.

Statistical analysis

Statistical analyses were performed with GraphPad Prism (version 4.03 for Windows; GraphPad Software, San Diego, Calif). Continuous normally distributed variables were expressed as mean ± SD. Dispersion indices had non-Gaussian distributions and were presented as median and interquartile range (IQR) (25th-75th percentile). Mean phases

were compared by use of paired *t* tests. Correlations between planar and tomographic dispersion estimates were made by use of Spearman coefficients. The relationship between these parameters was explored by nonlinear regression analyses based on a translated exponential. Comparisons between functional class and contraction analysis were performed by use of analysis of variance (Kruskal-Wallis test). A 2-tailed $P < .05$ was considered to indicate statistical significance.

RESULTS

Baseline characteristics

Overall, 235 patients (79% male; mean age, 62 ± 11 years) were recruited and successfully completed the study. The mean body mass index was 27.2 ± 4.6 kg/m^2. The following risk factors for CAD were noted: diabetes (n = 57), hypertension (n = 105), dyslipidemia (n = 132), active smoking (n = 47), and past history of smoking (n = 49). For the cardiac heart failure symptoms, functional class was evaluated with the New York Heart Association (NYHA) classification. Of the patients, 41 were in class I, 109 were in class II, and 42 were in class III.

LVEF

By the planar method, the LVEF ranged from 8% to 75%, with a mean LVEF of 33.5% ± 13.5%. By the 3D method, the mean LVEF was 34.7% ± 12.7%, which was not

statistically significantly different. As depicted in Figure 1, an excellent correlation was noted between the two methods *(r* = 0.83, *P* < .0001).

Phase angles

Mean phase angles for planar and tomographic methods were 126.3° ± 29.6° and 124.4° ± 28.7°, respectively, with a moderate correlation between the two *(r* = 0.53, *P* < .0001), as illustrated in Figures 2 and 3.

CHI and heterogeneity index

Phase and amplitude signals were incorporated in CHI, which had a median value of 73.8% (IQR, 58.7%-84.9%). The amplitude of the out-of-phase septal wall movement modulates the deleterious effect on global ventricular function. The negative impact of a dyskinetic wall segment is minimized if regional motion is limited.

The planar heterogeneity index (SDΦ) was 28.2° (IQR, 17.5°-46.8°), which inversely correlated with CHI *(r* = -0.61, *P* < .0001), as graphically displayed in Figure 4. In further analyses these dispersion indices were compared with LVEF. In planar mode an inverse relationship between dispersion index and LVEF was observed, as depicted in Figure 5. In contrast, a positive correlation between dispersion index and LVEF was noted with the 3D method, as illustrated in Figure 6. In both instances visual inspection of the graphs revealed a nonlinear relationship between dispersion index and LVEF. LVEF remained

proportional to CHI until a plateau was reached, after which no further increase in CHI was observed.

Comparisons between NYHA functional class and contraction homogeneity analysis are shown in Table 1. For the planar analysis (SDΦ), significant differences were only seen between NYHA class I and class III. However, for the 3D index (CHI), significant differences were observed between each functional class.

DISCUSSION

CRT is a relatively new treatment modality for patients with symptomatic heart failure resulting from systolic dysfunction. By simultaneously pacing both left and right ventricles in selected patients, the timing of global LV depolarization is synchronized, with improvements in mechanical contractility and mitral regurgitation. Early studies with CRT demonstrated its ability to improve symptoms, exercise capacity, and well-being of many patients with moderate to severe heart failure. Other studies demonstrated the capacity for CRT to reduce LV dilation and improve energy efficiency. Beneficial effects were borne out by large-scale randomized clinical trials. In eligible candidates the COMPANION (Comparison of Medical Therapy, Pacing, and Defibrillation in Chronic Heart Failure) study demonstrated a reduction in hospitalizations,[6] and the CARE-HF (Cardiac Resynchronization in Heart Failure) study documented a survival benefit.[7]

QRS duration has traditionally been used as an electrical marker of asynchrony and remains an inclusion criterion in many trials.[8] Nevertheless, several studies have noted that the magnitude of mechanical dyssynchrony is a more powerful predictor of ventricular function and response to CRT than QRS duration.[9] There is, therefore, much interest in developing a simple means of providing accurate and reproducible indices of cardiac dyssynchrony. In this study we present the theoretic concept of ventricular contraction efficiency as a 3D parameter with the potential to better quantify the impact of dyssynchrony on ventricular function.

On a practical level, CHI can serve as a single parameter that reflects global homogeneity of LV contraction. The concept of contraction efficiency considers the magnitude of effect of specific wall motion abnormalities, factoring in the notion that the impact of asynchronous wall motion relates not only to phase contraction delay but also to the amplitude of this delayed motion. An asynchronous segment of small amplitude has a lesser effect on global ventricular efficiency than asynchronous wall motion of greater amplitude. Also, our results exposed a better association between CHI and functional class compared with the planar parameter.

This concept overcomes some limitations of standard planar imaging, as a 2-dimensional representation provides only partial estimates of true synchrony. Indeed, in the best septal view, it is difficult to adequately assess anterior and inferior wall motion, as

the borders are not clearly visible. Moreover, all incidences provide partial information and may be considered incomplete.

In this study we found a correlation between LVEF and global ventricular synchrony computed by both planar and 3D methods. LVEF remained proportional to CHI until a plateau was reached (Figure 6). It may be conjectured that this point of deflection represents optimal synchrony and further increases in LVEF must be accounted for by other factors. Moreover, the presence of dyssynchrony does not necessarily imply a low LVEF. Conversely, a severely reduced LVEF does not inexorably generate substantial dyssynchrony, as hypokinesia may be homogeneous.

Fourier analysis was previously used to characterize conduction abnormalities[10-12] and to quantify cardiac wall motion with planar imaging.[13-16] Muramatsu et al[17] more recently applied Fourier analysis to blood pool SPECT imaging in assessing indications for CRT. However, the transformation was applied directly to blood pool images without segmentation, and phase rather than efficiency criteria were used. O'Connell et al[18] also reported phase and amplitude signals with planar imaging in a limited number of patients. Casset-Senon et al[19] applied Fourier analysis to SPECT data using a first harmonic model on a thick-slice blood pool model without segmentation. In the absence of prior segmentation, the amplitude of the Fourier signal on the endocardial border was related to variations in blood pool intensity. In contrast, when we applied Fourier analysis to leading edge–

detected points, amplitude signals were related to quantity of blood motion, which more directly and appropriately characterizes the physiologic process.

In the absence of a "gold standard," it is difficult to quantify true accuracy of the proposed technique. Sensitivity of the SD of the LV phase by the planar method has been previously assessed to detect segmental wall motion abnormalities.[16] This parameter independently predicted major cardiac events in patients with idiopathic dilated cardiomyopathy.[20] Other investigators have relied on planar estimates to predict response to CRT.[9] Our 3D assessment correlates reasonably well with planar mode values. It should be noted that a less-than-perfect correlation is not necessarily undesirable, given that full concordance would suggest a technique no better than its flawed counterpart. The ultimate utility of our technique remains to be ascertained in studies that correlate results with clinical endpoints.

We do, however, believe that the proposed CHI approach by use of GBP SPECT imaging offers several theoretic advantages over current methods. First, 3D quantification of ventricular synchrony overcomes inherent inaccuracies from 2-dimensional imaging. Second, automated data processing results in reductions in variability for repeated measures. Third, reliability of segmentation allows more precise definition of ventricular chambers, removing distorting effects from atrial contamination. Fourth, the effectiveness parameter overcomes difficulties arising from indeterminate phase imaging in the presence of akinesia or severe hypokinesia. Moreover, this novel parameter is intuitively appealing,

as it incorporates the pathophysiologic concept that high-amplitude out-of-phase contraction generates more deleterious effects on total ventricular dynamics and ejection volume than comparatively smaller out-of-phase hypokinesia. In comparison to echocardiographic indices, our proposed method is more expedient, as all processing is performed by computer software with data in 4-dimensional format (3D plus time). Finally, in keeping with the principle of parsimony, the mathematical equation remains simplistic and interpretable physiologically.

Perfusion myocardial imaging can be used for segmentation of the left ventricle and phase analysis of motion.[21-23] Blood pool imaging has the advantage of providing preserved endocardial edges even in the presence of wide myocardial scar. Moreover, right ventricular analysis can be performed, leading to interventricular delay computation. These analyses were already on hand, and the results will be the subject of a forthcoming publication. However, the ability to detect myocardial necrosis can be potentially useful to discriminate passive versus active movements.

The technique proposed may be further improved by refining its algorithms. For example, the first harmonic, though useful, remains an overly simplistic representation of a complex data set. Furthermore, cardiac contraction generates net movement of the entire heart (translation and rotation) that compounds individual segmental motion. This may result in apparent motion that does not accurately reflect cardiac systole. Although little quantitative

information exists on the contribution of such general movement to the overall effectiveness of ventricular contraction, the impact of global cardiac motion is likely small in comparison to myocardial contraction. Nevertheless, further analysis of these movements with careful distinction of contractile motion (ie, non-rigid vs rigid contraction analysis) may add further clarity and precision to measured estimates. Finally, an analysis of ventricular contraction before and after implantation of a biventricular pacemaker would be useful to characterize the effects of the resynchronization therapy. Animal studies are already on hand in a heart failure dog's model.

In conclusion, we describe a novel technique by which to assess ventricular dyssynchrony by means of 3D GBP SPECT imaging. This approach quantifies ventricular contraction efficiency and computes an intuitive CHI that considers both the phase delay of a dyssynchronous segment and its magnitude of contraction. Such detailed assessment should better characterize dynamics of ventricular contraction and elucidate the variable impact of dyssynchronous segments on global ventricular function. The ultimate utility of this approach awaits prospective clinical studies in selecting appropriate candidates for CRT, guiding lead placement, quantifying responses to CRT, and determining predictors of favorable outcomes.

Acknowledgment

The authors have indicated they have no financial conflicts of interest.

References

1. Abraham WT, Fisher WG, Smith AL, Delurgio DB, Leon AR, Loh E, et al. Cardiac resynchronization in chronic heart failure. N Engl J Med 2002;346:1845-53.
2. Auricchio A, Kloss M, Trautmann SI, Rodner S, Klein H. Exercise performance following cardiac resynchronization therapy in patients with heart failure and ventricular conduction delay. Am J Cardiol 2002;89:198-203.
3. Auricchio A, Stellbrink C, Sack S, Block M, Vogt J, Bakker P, et al. Long-term clinical effect of hemodynamically optimized cardiac resynchronization therapy in patients with heart failure and ventricular conduction delay. J Am Coll Cardiol 2002;39:2026-33.
4. Cazeau S, Leclercq C, Lavergne T, Walker S, Varma C, Linde C, et al. Effects of multisite biventricular pacing in patients with heart failure and intraventricular conduction delay. N Engl J Med 2001;344:873-80.
5. Harel F, Finnerty V, Ngo Q, Grégoire J, Khairy P, Thibault B. SPECT versus planar gated blood pool imaging for left ventricular evaluation. J Nucl Cardiol 2007;14:544-9.
6. Bristow MR, Saxon LA, Boehmer J, Krueger S, Kass DA, De Marco T, et al. Cardiac-resynchronization therapy with or without an implantable defibrillator in advanced chronic heart failure. N Engl J Med 2004;350:2140-50.
7. Cleland JG, Daubert JC, Erdmann E, Freemantle N, Gras D, Kappenberger L, et al. The effect of cardiac resynchronization on morbidity and mortality in heart failure. N Engl J Med 2005;352: 1539-49.

8. Swedberg K, Cleland J, Dargie H, Drexler H, Follath F, Komajda M, et al. Guidelines for the diagnosis and treatment of chronic heart failure: executive summary (update 2005) [in Spanish]. Rev Esp Cardiol 2005;58:1062-92.

9. Breithardt OA, Stellbrink C, Kramer AP, Sinha AM, Franke A, Salo R, et al. Echocardiographic quantification of left ventricular asynchrony predicts an acute hemodynamic benefit of cardiac resynchronization therapy. J Am Coll Cardiol 2002;40:536-45.

10. Botvinick EH, Frais MA, Shosa DW, O'Connell JW, Pacheco-Alvarez JA, Scheinman M, et al. An accurate means of detecting and characterizing abnormal patterns of ventricular activation by phase image analysis. Am J Cardiol 1982;50:289-98.

11. Links JM, Raichlen JS, Wagner HN Jr, Reid PR. Assessment of the site of ventricular activation by Fourier analysis of gated bloodpool studies. J Nucl Med 1985;26:27-32.

12. Raichlen JS, Links JM, Reid PR. Effect of electrical activation site on left ventricular performance in ventricular tachycardia patients with coronary heart disease. Am J Cardiol 1985;55:84-8.

13. Botvinick E, Dunn R, Frais M, O'Connell W, Shosa D, Herfkens R, et al. The phase image: its relationship to patterns of contraction and conduction. Circulation 1982;65:551-60.

14. Brateman L, Buckley K, Keim SG, Wargovich TJ, Williams CM. Left ventricular regional wall motion assessment by radionuclide ventriculography: a comparison of cine display with Fourier imaging. J Nucl Med 1991;32:777-82.

15. Mancini GB, Peck WW, Slutsky RA. Analysis of phase-angle histograms from equilibrium radionuclide studies: correlation with semiquantitative grading of wall motion. Am J Cardiol 1985;55: 535-40.

16. Vos PH, Vossepoel AM, Pauwels EK. Quantitative assessment of wall motion in multiple-gated studies using temporal Fourier analysis. J Nucl Med 1983;24:388-96.

17. Muramatsu T, Matsumoto K, Nishimura S. Efficacy of the phase images in Fourier analysis using gated cardiac POOL-SPECT for determining the indication for cardiac resynchronization therapy. Circ J 2005;69:1521-6.

18. O'Connell JW, Schreck C, Moles M, Badwar N, DeMarco T, Olgin J, et al. A unique method by which to quantitate synchrony with equilibrium radionuclide angiography. J Nucl Cardiol 2005; 12:441-50.

19. Casset-Senon D, Babuty D, Philippe L, Fauchier L, Eder V, Fauchier JP, et al. Fourier phase analysis of SPECT equilibrium radionuclide angiography in symptomatic patients with mitral valve prolapse without significant mitral regurgitation: assessment of biventricular functional abnormalities suggesting a cardiomyopathy. J Nucl Cardiol 2000;7:471-7.

20. Fauchier L, Marie O, Casset-Senon D, Babuty D, Cosnay P, Fauchier JP. Interventricular and intraventricular dyssynchrony in idiopathic dilated cardiomyopathy:

a prognostic study with Fourier phase analysis of radionuclide angioscintigraphy. J Am Coll Cardiol 2002;40:2022-30.

21. Chen J, Garcia EV, Folks RD, Cooke CD, Faber TL, Tauxe EL, et al. Onset of left ventricular mechanical contraction as determined by phase analysis of ECG-gated myocardial perfusion SPECT imaging: development of a diagnostic tool for assessment of cardiac mechanical dyssynchrony. J Nucl Cardiol 2005;12:687-95.

22. Henneman MM, Chen J, Ypenburg C, Dibbets P, Bleeker GB, Boersma E, et al. Phase analysis of gated myocardial perfusion single-photon emission computed tomography compared with tissue Doppler imaging for the assessment of left ventricular dyssynchrony. J Am Coll Cardiol 2007;49:1708-14.

23. Trimble MA, Borges-Neto S, Smallheiser S, Chen J, Honeycutt EF, Shaw LK, et al. Evaluation of left ventricular mechanical dyssynchrony as determined by phase analysis of ECG-gated SPECT myocardial perfusion imaging in patients with left ventricular dysfunction and conduction disturbances. J Nucl Cardiol 2007;14:298-307.

Figures

Figure 1. Regression analyses showing associations between invariance-of-Laplacian method (3D) and planar method for LVEF computation.

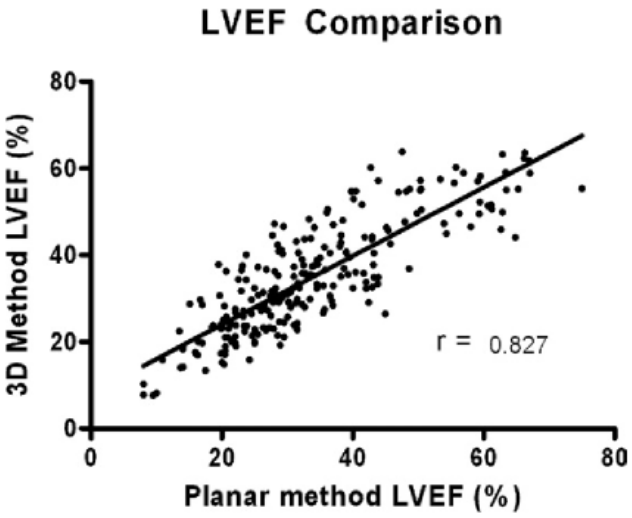

Figure 2. Histogram showing frequency of LV mean phase computed by invariance-of-Laplacian method *(green bars; 3D)* and planar algorithm *(red bars)*.

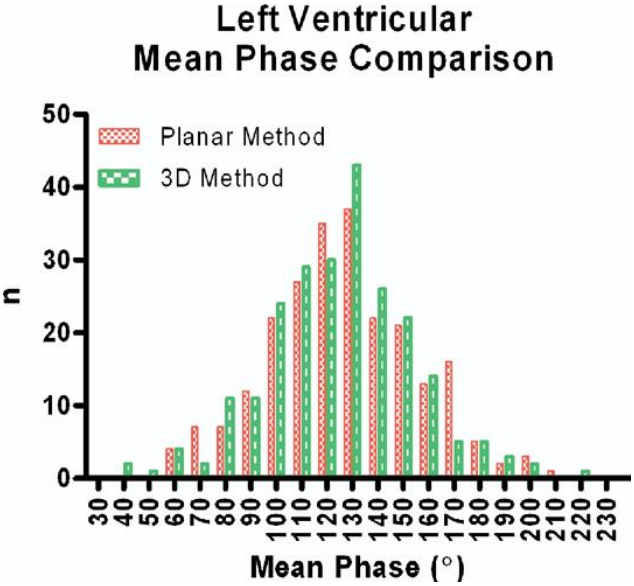

Figure 3. Regression analysis showing correlation for LV mean phase computed by invariance-of-Laplacian (3D) and planar methods.

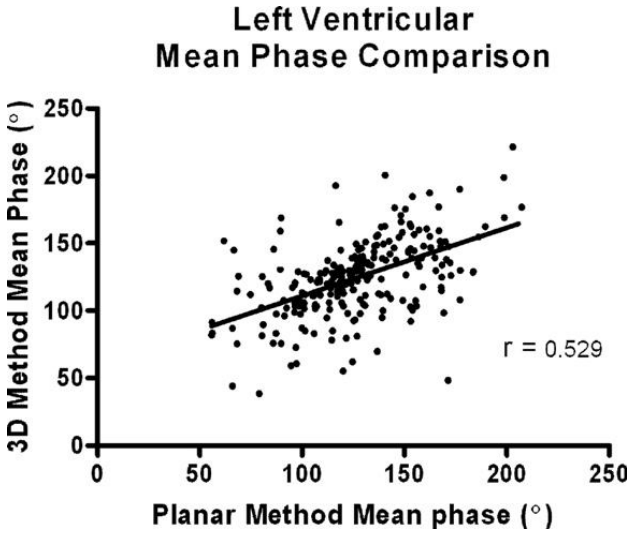

Figure 4. Scatter plot with regression analyses of dispersion index.

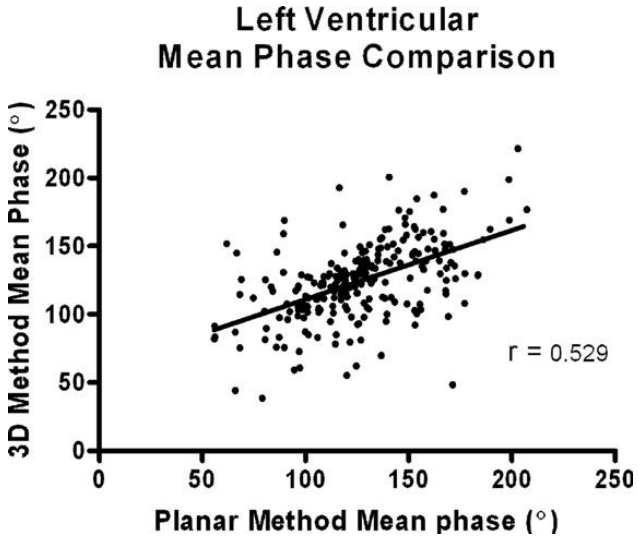

Figure 5. Scatter plot showing relation between planar dispersion index (SDΦ) and LVEF.

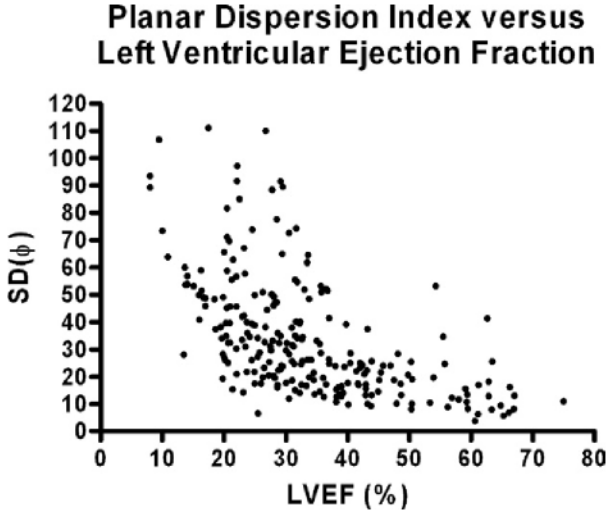

Figure 6. Scatter plot showing relation between 3D dispersion index (CHI) and LVEF.

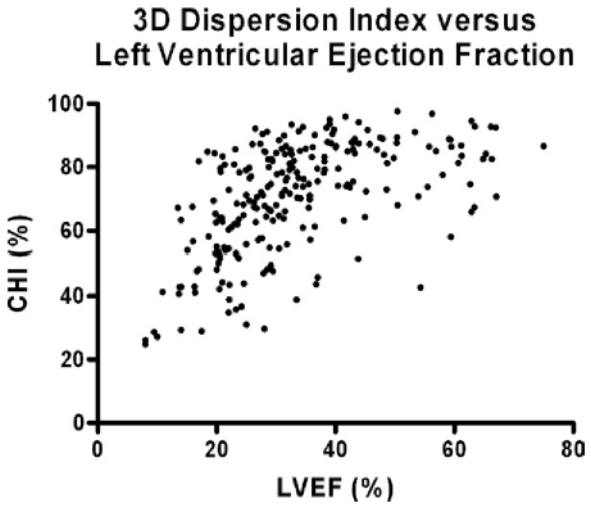

Table 1. Comparisons between NYHA functional class and contraction homogeneity analysis

	NYHA functional class		
	I	**II**	**III**
SDΦ (°)	25.94 ± 15.02	32.35 ± 18.49	44.60 ± 28.42*
CHI (%)	78.01 ± 12.48†	70.76 ± 16.22	61.52 ± 19.75‡

Data are given as mean ± SD.

*P < .05 for comparison between class I and class III.

†P < .05 for comparison between class I and class II.

‡P < .05 for comparison between class II and class III and between class I and class III.

Conclusion

La cardiologie nucléaire demeure une spécialité d'actualité et en constante progression. Cette discipline a démontré des avancements majeurs depuis sa création, notamment dans l'évaluation de la perfusion et de la fonction myocardique. Par ailleurs, les opportunités de développer de nouvelles applications reliées au système cardiovasculaire méritent d'être signalées et encouragées.

L'évaluation non-invasive de la fonction endothéliale représente une 'quête' attrayante pour de nombreux groupes de recherche et leurs partenaires commerciaux respectifs. Différentes approches ont été expérimentées avec plus ou moins de succès. Un compromis est essentiel à obtenir entre la spécificité du signal mesuré et le caractère invasif de la procédure. L'échographie brachiale représente une méthodologie reconnue, possédant une reconnaissance scientifique certaine. Malgré cela, cette technique souffre de faiblesses avérées qui sont entre autres liées à sa complexité d'utilisation, à la nécessité d'un opérateur entraîné et au temps requis pour effectuer l'examen. Pour toutes ces raisons, l'échographie brachiale ne sera jamais une méthode de dépistage à grande échelle et ne pourra jamais être utilisée en prévention primaire.

Les nouvelles méthodologies proposées dans ce mémoire, tout en apportant des alternatives valables, soulèvent des questionnements quant à la compréhension des phénomènes vasculaires étudiés. En effet, la réaction hyperémique post-ischémique revêt

un caractère complexe, étant composé de multiples réactions locales, grossièrement classées en deux catégories: endothéliale-dépendante et endothéliale-indépendante. De plus, chacune de ces catégories inclut une panoplie d'évènements distincts, liés à l'intégrité endothéliale locale et aux multiples facteurs vaso-actifs impliqués dans l'homéostase vasculaire.

La pléthysmographie isotopique et son pendant utilisant la spectrographie infrarouge, fournissent des procédés de quantification pouvant être utilisés de façon répandue. L'automatisation du système de mesure permet l'usage de la technique par un personnel non spécialisé tout en maintenant une qualité et reproductibilité adéquates des signaux obtenus. De plus, la technique par spectroscopie ne nécessite aucune injection de substance exogène.

Par ailleurs, l'asynchronisme de contraction ventriculaire représente un sujet d'actualité depuis les succès de la thérapie de resynchronisation chez les patients porteurs d'insuffisance cardiaque non-contrôlée médicalement.

La compréhension du phénomène physiopathologique a progressée au rythme des capacités d'observation et d'analyse du phénomène étudié. En effet, l'idée première voulant que la majoration de la fonction ventriculaire gauche soit obtenue principalement par la resynchronisation auriculoventriculaire a été rapidement abandonnée. Après un bref intérêt portant sur l'asynchronisme interventriculaire, la majorité des groupes de recherche ont fondé leurs espoirs sur la caractérisation du délai intraventriculaire et son importance

comme cause d'aggravation de la défaillance ventriculaire gauche. La nouvelle méthodologie proposée permet de mieux situer les contributions des différents facteurs impliqués dans cette pathologie. En permettant la caractérisation de l'asynchronisme intra- et interventriculaire et en procurant des estimations précises de la fonction ventriculaire gauche (volumes et FEVG), la nouvelle méthodologie permet d'optimiser la sélection des patients pouvant obtenir des bénéfices à la CRT tout en unifiant les méthodologies de mesures servant à quantifier l'asynchronisme d'une part, et valider la réponse à la resynchronisation d'autre part.

L'usage de l'imagerie isotopique de type SPECT permet la caractérisation de la dynamique cardiaque sur l'ensemble des parois des deux ventricules et ce d'une façon totalement simultanée. La contemporanéité de l'ensemble des données couplées à la qualité de l'échantillonnage spatial permet une analyse précise et fiable de l'asynchronisme intra- et inter-ventriculaire. Cette approche permet également une mesure fiable et précise des volumes ventriculaires, paramètres de plus en plus utilisés comme point d'aboutissement des études portant sur les bénéfices de la resynchronisation cardiaque. La sélection optimale des patients comportant des critères de réponse favorable à la CRT ne peut être effectuée qu'en étudiant de façon précise le comportement segmentaire et global de la dynamique de contraction ventriculaire. La méthodologie proposée permet cette analyse et nous croyons qu'elle peut permettre une meilleure compréhension des phénomènes impliqués. Par contre, selon moi, une meilleure compréhension fera apparaître un niveau

supérieur de complexité et d'interrelation entre de nouveaux cofacteurs, nécessitant de poursuivre les recherches dans ce domaine.

Bibliographie

1. Shaw LJ, Hachamovitch R, Heller GV, Marwick TH, Travin MI, Iskandrian AE, et al. Noninvasive strategies for the estimation of cardiac risk in stable chest pain patients. The Economics of Noninvasive Diagnosis (END) Study Group. Am J Cardiol 2000;86(1):1-7.
2. Shaw LJ, Berman DS, Maron DJ, Mancini GB, Hayes SW, Hartigan PM, et al. Optimal medical therapy with or without percutaneous coronary intervention to reduce ischemic burden: results from the Clinical Outcomes Utilizing Revascularization and Aggressive Drug Evaluation (COURAGE) trial nuclear substudy. Circulation 2008;117(10):1283-91.
3. Blumgart HL, Weiss S. STUDIES ON THE VELOCITY OF BLOOD FLOW: VII. The Pulmonary Circulation Time in Normal Resting Individuals. J Clin Invest 1927;4(3):399-425.
4. Prinzmetal M, Corday E, et al. Radiocardiography and its clinical applications. J Am Med Assoc 1949;139(10):617-22.
5. Anger HO. A multiple scintillation counter in vivo scanner. Am J Roentgenol Radium Ther Nucl Med 1953;70(4):605-12.
6. Askenazi J, Ahnberg DS, Korngold E, LaFarge CG, Maltz DL, Treves S. Quantitative radionuclide angiocardiography: detection and quantitation of left to right shunts. Am J Cardiol 1976;37(3):382-7.
7. Kriss JP, Enright LP, Hayden WG, Wexler L, Shumway NE. Radioisotopic angiocardiography. Wide scope of applicability in diagnosis and evaluation of therapy in diseases of the heart and great vessels. Circulation 1971;43(6):792-808.
8. Schelbert HR, Verba JW, Johnson AD, Brock GW, Alazraki NP, Rose FJ, et al. Nontraumatic determination of left ventricular ejection fraction by radionuclide angiocardiography. Circulation 1975;51(5):902-9.
9. Strauss HW, Zaret BL, Hurley PJ, Natarajan TK, Pitt B. A scintiphotographic method for measuring left ventricular ejection fraction in man without cardiac catheterization. Am J Cardiol 1971;28(5):575-80.
10. Zaret BL, Strauss HW, Hurley PJ, Natarajan TK, Pitt B. A noninvasive scintiphotographic method for detecting regional ventricular dysfunction in man. N Engl J Med 1971;284(21):1165-70.
11. Schwartz RG, McKenzie WB, Alexander J, Sager P, D'Souza A, Manatunga A, et al. Congestive heart failure and left ventricular dysfunction complicating doxorubicin therapy. Seven-year experience using serial radionuclide angiocardiography. Am J Med 1987;82(6):1109-18.
12. Borer JS, Bacharach SL, Green MV, Kent KM, Epstein SE, Johnston GS. Real-time radionuclide cineangiography in the noninvasive evaluation of global and regional left ventricular function at rest and during exercise in patients with coronary-artery disease. N Engl J Med 1977;296(15):839-44.
13. Bradley-Moore PR, Lebowitz E, Greene MW, Atkins HL, Ansari AN. Thallium-201 for medical use. II: Biologic behavior. J Nucl Med 1975;16(2):156-60.

14. Lebowitz E, Greene MW, Fairchild R, Bradley-Moore PR, Atkins HL, Ansari AN, et al. Thallium-201 for medical use. I. J Nucl Med 1975;16(2):151-5.
15. Pohost GM, Zir LM, Moore RH, McKusick KA, Guiney TE, Beller GA. Differentiation of transiently ischemic from infarcted myocardium by serial imaging after a single dose of thallium-201. Circulation 1977;55(2):294-302.
16. Holman BL, Jones AG, Lister-James J, Davison A, Abrams MJ, Kirshenbaum JM, et al. A new Tc-99m-labeled myocardial imaging agent, hexakis(t-butylisonitrile)-technetium(I) [Tc-99m TBI]: initial experience in the human. J Nucl Med 1984;25(12):1350-5.
17. Seldin DW, Johnson LL, Blood DK, Muschel MJ, Smith KF, Wall RM, et al. Myocardial perfusion imaging with technetium-99m SQ30217: comparison with thallium-201 and coronary anatomy. J Nucl Med 1989;30(3):312-9.
18. Zaret BL, Rigo P, Wackers FJ, Hendel RC, Braat SH, Iskandrian AS, et al. Myocardial perfusion imaging with 99mTc tetrofosmin. Comparison to 201Tl imaging and coronary angiography in a phase III multicenter trial. Tetrofosmin International Trial Study Group. Circulation 1995;91(2):313-9.
19. Elhendy A, Bax JJ, Poldermans D. Dobutamine stress myocardial perfusion imaging in coronary artery disease. J Nucl Med 2002;43(12):1634-46.
20. Elhendy A, Geleijnse ML, Roelandt JR, van Domburg RT, Nierop PR, Bax JJ, et al. Dobutamine 99Tcm-MIBI SPET myocardial perfusion scintigraphy in the prediction of restenosis after percutaneous transluminal coronary angioplasty in patients unable to perform an exercise stress test. Nucl Med Commun 1997;18(2):122-8.
21. Geleijnse ML, Elhendy A, Fioretti PM, Roelandt JR. Dobutamine stress myocardial perfusion imaging. J Am Coll Cardiol 2000;36(7):2017-27.
22. Gould KL. Assessment of coronary stenoses with myocardial perfusion imaging during pharmacologic coronary vasodilatation. IV. Limits of detection of stenosis with idealized experimental cross-sectional myocardial imaging. Am J Cardiol 1978;42(5):761-8.
23. Hendel RC, Bateman TM, Cerqueira MD, Iskandrian AE, Leppo JA, Blackburn B, et al. Initial clinical experience with regadenoson, a novel selective A2A agonist for pharmacologic stress single-photon emission computed tomography myocardial perfusion imaging. J Am Coll Cardiol 2005;46(11):2069-75.
24. Iskandrian AE, Bateman TM, Belardinelli L, Blackburn B, Cerqueira MD, Hendel RC, et al. Adenosine versus regadenoson comparative evaluation in myocardial perfusion imaging: results of the ADVANCE phase 3 multicenter international trial. J Nucl Cardiol 2007;14(5):645-58.
25. Berman DS, Hachamovitch R, Shaw LJ, Friedman JD, Hayes SW, Thomson LE, et al. Roles of nuclear cardiology, cardiac computed tomography, and cardiac magnetic resonance: assessment of patients with suspected coronary artery disease. J Nucl Med 2006;47(1):74-82.
26. Fuster V. Hurst's the heart. 12th ed. New York: McGraw-Hill Medical; 2008.
27. Brunken R, Tillisch J, Schwaiger M, Child JS, Marshall R, Mandelkern M, et al. Regional perfusion, glucose metabolism, and wall motion in patients with chronic

electrocardiographic Q wave infarctions: evidence for persistence of viable tissue in some infarct regions by positron emission tomography. Circulation 1986;73(5):951-63.
28. Tillisch J, Brunken R, Marshall R, Schwaiger M, Mandelkern M, Phelps M, et al. Reversibility of cardiac wall-motion abnormalities predicted by positron tomography. N Engl J Med 1986;314(14):884-8.
29. Celermajer DS. Endothelial dysfunction: does it matter? Is it reversible? J Am Coll Cardiol 1997;30(2):325-33.
30. Schachinger V, Britten MB, Zeiher AM. Prognostic impact of coronary vasodilator dysfunction on adverse long-term outcome of coronary heart disease. Circulation 2000;101(16):1899-906.
31. Verma S, Anderson TJ. Fundamentals of endothelial function for the clinical cardiologist. Circulation 2002;105(5):546-9.
32. Vanhoutte PM. Endothelium and control of vascular function. State of the Art lecture. Hypertension 1989;13(6 Pt 2):658-67.
33. Raitakari OT, Celermajer DS. Testing for endothelial dysfunction. Ann Med 2000;32(5):293-304.
34. Gaeta G, De Michele M, Cuomo S, Guarini P, Foglia MC, Bond MG, et al. Arterial abnormalities in the offspring of patients with premature myocardial infarction. N Engl J Med 2000;343(12):840-6.
35. Rubanyi GM. The role of endothelium in cardiovascular homeostasis and diseases. J Cardiovasc Pharmacol 1993;22 Suppl 4:S1-14.
36. Ross R. The pathogenesis of atherosclerosis: a perspective for the 1990s. Nature 1993;362(6423):801-9.
37. Zeiher AM, Krause T, Schachinger V, Minners J, Moser E. Impaired endothelium-dependent vasodilation of coronary resistance vessels is associated with exercise-induced myocardial ischemia. Circulation 1995;91(9):2345-52.
38. Gould KL, Martucci JP, Goldberg DI, Hess MJ, Edens RP, Latifi R, et al. Short-term cholesterol lowering decreases size and severity of perfusion abnormalities by positron emission tomography after dipyridamole in patients with coronary artery disease. A potential noninvasive marker of healing coronary endothelium. Circulation 1994;89(4):1530-8.
39. Eichstadt HW, Eskotter H, Hoffman I, Amthauer HW, Weidinger G. Improvement of myocardial perfusion by short-term fluvastatin therapy in coronary artery disease. Am J Cardiol 1995;76(2):122A-125A.
40. Baller D, Notohamiprodjo G, Gleichmann U, Holzinger J, Weise R, Lehmann J. Improvement in coronary flow reserve determined by positron emission tomography after 6 months of cholesterol-lowering therapy in patients with early stages of coronary atherosclerosis. Circulation 1999;99(22):2871-5.
41. de Divitiis M, Rubba P, Di Somma S, Liguori V, Galderisi M, Montefusco S, et al. Effects of short-term reduction in serum cholesterol with simvastatin in patients with stable angina pectoris and mild to moderate hypercholesterolemia. Am J Cardiol 1996;78(7):763-8.

42. Czernin J, Barnard RJ, Sun KT, Krivokapich J, Nitzsche E, Dorsey D, et al. Effect of short-term cardiovascular conditioning and low-fat diet on myocardial blood flow and flow reserve. Circulation 1995;92(2):197-204.
43. Gould KL, Ornish D, Scherwitz L, Brown S, Edens RP, Hess MJ, et al. Changes in myocardial perfusion abnormalities by positron emission tomography after long-term, intense risk factor modification. Jama 1995;274(11):894-901.
44. Schuler G, Hambrecht R, Schlierf G, Grunze M, Methfessel S, Hauer K, et al. Myocardial perfusion and regression of coronary artery disease in patients on a regimen of intensive physical exercise and low fat diet. J Am Coll Cardiol 1992;19(1):34-42.
45. Randomised trial of cholesterol lowering in 4444 patients with coronary heart disease: the Scandinavian Simvastatin Survival Study (4S). Lancet 1994;344(8934):1383-9.
46. Blankenhorn DH, Azen SP, Kramsch DM, Mack WJ, Cashin-Hemphill L, Hodis HN, et al. Coronary angiographic changes with lovastatin therapy. The Monitored Atherosclerosis Regression Study (MARS). The MARS Research Group. Ann Intern Med 1993;119(10):969-76.
47. Ludmer PL, Selwyn AP, Shook TL, Wayne RR, Mudge GH, Alexander RW, et al. Paradoxical vasoconstriction induced by acetylcholine in atherosclerotic coronary arteries. N Engl J Med 1986;315(17):1046-51.
48. Vita JA, Treasure CB, Nabel EG, McLenachan JM, Fish RD, Yeung AC, et al. Coronary vasomotor response to acetylcholine relates to risk factors for coronary artery disease. Circulation 1990;81(2):491-7.
49. Creager MA, Cooke JP, Mendelsohn ME, Gallagher SJ, Coleman SM, Loscalzo J, et al. Impaired vasodilation of forearm resistance vessels in hypercholesterolemic humans. J Clin Invest 1990;86(1):228-34.
50. Panza JA, Quyyumi AA, Brush JE, Jr., Epstein SE. Abnormal endothelium-dependent vascular relaxation in patients with essential hypertension. N Engl J Med 1990;323(1):22-7.
51. Duffy SJ, New G, Tran BT, Harper RW, Meredith IT. Relative contribution of vasodilator prostanoids and NO to metabolic vasodilation in the human forearm. Am J Physiol 1999;276(2 Pt 2):H663-70.
52. Meredith IT, Currie KE, Anderson TJ, Roddy MA, Ganz P, Creager MA. Postischemic vasodilation in human forearm is dependent on endothelium-derived nitric oxide. Am J Physiol 1996;270(4 Pt 2):H1435-40.
53. Donohue TJ, Miller DD, Bach RG, Tron C, Wolford T, Caracciolo EA, et al. Correlation of poststenotic hyperemic coronary flow velocity and pressure with abnormal stress myocardial perfusion imaging in coronary artery disease. Am J Cardiol 1996;77(11):948-54.
54. Gould KL, Nakagawa Y, Nakagawa K, Sdringola S, Hess MJ, Haynie M, et al. Frequency and clinical implications of fluid dynamically significant diffuse coronary artery disease manifest as graded, longitudinal, base-to-apex myocardial perfusion abnormalities by noninvasive positron emission tomography. Circulation 2000;101(16):1931-9.
55. Hausmann D, Johnson JA, Sudhir K, Mullen WL, Friedrich G, Fitzgerald PJ, et al. Angiographically silent atherosclerosis detected by intravascular ultrasound in patients with

familial hypercholesterolemia and familial combined hyperlipidemia: correlation with high density lipoproteins. J Am Coll Cardiol 1996;27(7):1562-70.
56. Voudris V, Manginas A, Vassilikos V, Koutelou M, Kantzis J, Cokkinos DV. Coronary flow velocity changes after intravenous dipyridamole infusion: measurements using intravascular Doppler guide wire. A documentation of flow inhomogeneity. J Am Coll Cardiol 1996;27(5):1148-55.
57. Fayad ZA, Fuster V, Fallon JT, Jayasundera T, Worthley SG, Helft G, et al. Noninvasive in vivo human coronary artery lumen and wall imaging using black-blood magnetic resonance imaging. Circulation 2000;102(5):506-10.
58. Botnar RM, Stuber M, Kissinger KV, Kim WY, Spuentrup E, Manning WJ. Noninvasive coronary vessel wall and plaque imaging with magnetic resonance imaging. Circulation 2000;102(21):2582-7.
59. Hatsukami TS, Ross R, Polissar NL, Yuan C. Visualization of fibrous cap thickness and rupture in human atherosclerotic carotid plaque in vivo with high-resolution magnetic resonance imaging. Circulation 2000;102(9):959-64.
60. Joannides R, Haefeli WE, Linder L, Richard V, Bakkali EH, Thuillez C, et al. Nitric oxide is responsible for flow-dependent dilatation of human peripheral conduit arteries in vivo. Circulation 1995;91(5):1314-9.
61. Chen CH, Ting CT, Nussbacher A, Nevo E, Kass DA, Pak P, et al. Validation of carotid artery tonometry as a means of estimating augmentation index of ascending aortic pressure. Hypertension 1996;27(2):168-75.
62. Kelly R, Hayward C, Avolio A, O'Rourke M. Noninvasive determination of age-related changes in the human arterial pulse. Circulation 1989;80(6):1652-9.
63. Hayward CS, Kelly RP. Gender-related differences in the central arterial pressure waveform. J Am Coll Cardiol 1997;30(7):1863-71.
64. Roman MJ, Pini R, Pickering TG, Devereux RB. Non-invasive measurements of arterial compliance in hypertensive compared with normotensive adults. J Hypertens Suppl 1992;10(6):S115-8.
65. Vaitkevicius PV, Fleg JL, Engel JH, O'Connor FC, Wright JG, Lakatta LE, et al. Effects of age and aerobic capacity on arterial stiffness in healthy adults. Circulation 1993;88(4 Pt 1):1456-62.
66. Hayward CS, Kraidly M, Webb CM, Collins P. Assessment of endothelial function using peripheral waveform analysis: a clinical application. J Am Coll Cardiol 2002;40(3):521-8.
67. Chouraqui P, Schnall RP, Dvir I, Rozanski A, Qureshi E, Arditti A, et al. Assessment of peripheral artery tonometry in the detection of treadmill exercise-induced myocardial ischemia. J Am Coll Cardiol 2002;40(12):2195-200.
68. Liang YL, Teede H, Kotsopoulos D, Shiel L, Cameron JD, Dart AM, et al. Non-invasive measurements of arterial structure and function: repeatability, interrelationships and trial sample size. Clin Sci (Lond) 1998;95(6):669-79.
69. Schelbert HR. Positron emission tomography and the changing paradigm in coronary artery disease. Z Kardiol 2000;89(Suppl 4):IV55-60.

70. Yokoyama I, Ohtake T, Momomura S, Nishikawa J, Sasaki Y, Omata M. Reduced coronary flow reserve in hypercholesterolemic patients without overt coronary stenosis. Circulation 1996;94(12):3232-8.
71. Pitkanen OP, Nuutila P, Raitakari OT, Porkka K, Iida H, Nuotio I, et al. Coronary flow reserve in young men with familial combined hyperlipidemia. Circulation 1999;99(13):1678-84.
72. Pitkanen OP, Raitakari OT, Niinikoski H, Nuutila P, Iida H, Voipio-Pulkki LM, et al. Coronary flow reserve is impaired in young men with familial hypercholesterolemia. J Am Coll Cardiol 1996;28(7):1705-11.
73. Laine H, Raitakari OT, Niinikoski H, Pitkanen OP, Iida H, Viikari J, et al. Early impairment of coronary flow reserve in young men with borderline hypertension. J Am Coll Cardiol 1998;32(1):147-53.
74. Raitakari OT, Pitkanen OP, Lehtimaki T, Lahdenpera S, Iida H, Yla-Herttuala S, et al. In vivo low density lipoprotein oxidation relates to coronary reactivity in young men. J Am Coll Cardiol 1997;30(1):97-102.
75. Pitkanen OP, Raitakari OT, Ronnemaa T, Niinikoski H, Nuutila P, Iida H, et al. Influence of cardiovascular risk status on coronary flow reserve in healthy young men. Am J Cardiol 1997;79(12):1690-2.
76. Rubanyi GM, Romero JC, Vanhoutte PM. Flow-induced release of endothelium-derived relaxing factor. Am J Physiol 1986;250(6 Pt 2):H1145-9.
77. Dilsizian V. The role of myocardial perfusion imaging in vascular endothelial dysfunction. J Nucl Cardiol 2000;7(2):180-4.
78. Fujita H, Yamabe H, Yokoyama M. Effect of L-arginine administration on myocardial thallium-201 perfusion during exercise in patients with angina pectoris and normal coronary angiograms. J Nucl Cardiol 2000;7(2):97-102.
79. Moore JC, Baker CH. Red cell and albumin flow circuits during skeletal muscle reactive hyperemia. Am J Physiol 1971;220(5):1213-9.
80. Parkin A, Smye SW, Bishop N, Wilkinson D, Rees M, Vowden P, et al. Forearm blood flow measurements using technetium-99m human serum albumin following brachial arteriotomy. J Nucl Med 1989;30(1):45-50.
81. Dupuis J, Arsenault A, Meloche B, Harel F, Staniloae C, Grégoire J. Quantitative Hyperemic Reactivity in Opposed Limbs During Myocardial Perfusion Imaging: A New Marker of Coronary Artery Disease (in press). JACC 2004.
82. Lepage S. Acute decompensated heart failure. Can J Cardiol 2008;24 Suppl B:6B-8B.
83. Tsuyuki RT, Shibata MC, Nilsson C, Hervas-Malo M. Contemporary burden of illness of congestive heart failure in Canada. Can J Cardiol 2003;19(4):436-8.
84. Ho KK, Pinsky JL, Kannel WB, Levy D. The epidemiology of heart failure: the Framingham Study. J Am Coll Cardiol 1993;22(4 Suppl A):6A-13A.
85. Grines CL, Bashore TM, Boudoulas H, Olson S, Shafer P, Wooley CF. Functional abnormalities in isolated left bundle branch block. The effect of interventricular asynchrony. Circulation 1989;79(4):845-53.
86. Hultgren HN, Craige E, Fujii J, Nakamura T, Bilisoly J. Left bundle branch block and mechanical events of the cardiac cycle. Am J Cardiol 1983;52(7):755-62.

87. Sadaniantz A, Saint Laurent L. Left ventricular Doppler diastolic filling patterns in patients with isolated left bundle branch block. Am J Cardiol 1998;81(5):643-5.
88. Xiao HB, Lee CH, Gibson DG. Effect of left bundle branch block on diastolic function in dilated cardiomyopathy. Br Heart J 1991;66(6):443-7.
89. Baldasseroni S, Opasich C, Gorini M, Lucci D, Marchionni N, Marini M, et al. Left bundle-branch block is associated with increased 1-year sudden and total mortality rate in 5517 outpatients with congestive heart failure: a report from the Italian network on congestive heart failure. Am Heart J 2002;143(3):398-405.
90. Aaronson KD, Schwartz JS, Chen TM, Wong KL, Goin JE, Mancini DM. Development and prospective validation of a clinical index to predict survival in ambulatory patients referred for cardiac transplant evaluation. Circulation 1997;95(12):2660-7.
91. Bramlet DA, Morris KG, Coleman RE, Albert D, Cobb FR. Effect of rate-dependent left bundle branch block on global and regional left ventricular function. Circulation 1983;67(5):1059-65.
92. Kingma I, Tyberg JV, Smith ER. Effects of diastolic transseptal pressure gradient on ventricular septal position and motion. Circulation 1983;68(6):1304-14.
93. Ono S, Nohara R, Kambara H, Okuda K, Kawai C. Regional myocardial perfusion and glucose metabolism in experimental left bundle branch block. Circulation 1992;85(3):1125-31.
94. Zanco P, Desideri A, Mobilia G, Cargnel S, Milan E, Celegon L, et al. Effects of left bundle branch block on myocardial FDG PET in patients without significant coronary artery stenoses. J Nucl Med 2000;41(6):973-7.
95. Askenazi J, Alexander JH, Koenigsberg DI, Belic N, Lesch M. Alteration of left ventricular performance by left bundle branch block simulated with atrioventricular sequential pacing. Am J Cardiol 1984;53(1):99-104.
96. Gilmore JP, Sarnoff SJ, Mitchell JH, Linden RJ. Synchronicity of ventricular contraction: observations comparing haemodynamic effects of atrial and ventricular pacing. Br Heart J 1963;25:299-307.
97. Park RC, Little WC, O'Rourke RA. Effect of alteration of left ventricular activation sequence on the left ventricular end-systolic pressure-volume relation in closed-chest dogs. Circ Res 1985;57(5):706-17.
98. Zile MR, Blaustein AS, Shimizu G, Gaasch WH. Right ventricular pacing reduces the rate of left ventricular relaxation and filling. J Am Coll Cardiol 1987;10(3):702-9.
99. Coats AJ. MADIT II, the Multi-center Autonomic Defibrillator Implantation Trial II stopped early for mortality reduction, has ICD therapy earned its evidence-based credentials? Int J Cardiol 2002;82(1):1-5.
100. Connolly SJ, Gent M, Roberts RS, Dorian P, Roy D, Sheldon RS, et al. Canadian implantable defibrillator study (CIDS) : a randomized trial of the implantable cardioverter defibrillator against amiodarone. Circulation 2000;101(11):1297-302.
101. Connolly SJ, Hallstrom AP, Cappato R, Schron EB, Kuck KH, Zipes DP, et al. Meta-analysis of the implantable cardioverter defibrillator secondary prevention trials. AVID, CASH and CIDS studies. Antiarrhythmics vs Implantable Defibrillator study.

Cardiac Arrest Study Hamburg . Canadian Implantable Defibrillator Study. Eur Heart J 2000;21(24):2071-8.
102. Gold MR, Nisam S. Primary prevention of sudden cardiac death with implantable cardioverter defibrillators: lessons learned from MADIT and MUSTT. Pacing Clin Electrophysiol 2000;23(11 Pt 2):1981-5.
103. Moss AJ, Daubert J, Zareba W. MADIT-II: clinical implications. Card Electrophysiol Rev 2002;6(4):463-5.
104. Prystowsky EN, Nisam S. Prophylactic implantable cardioverter defibrillator trials: MUSTT, MADIT, and beyond. Multicenter Unsustained Tachycardia Trial. Multicenter Automatic Defibrillator Implantation Trial. Am J Cardiol 2000;86(11):1214-5, A5.
105. Linde C, Gadler F, Edner M, Nordlander R, Rosenqvist M, Ryden L. Results of atrioventricular synchronous pacing with optimized delay in patients with severe congestive heart failure. Am J Cardiol 1995;75(14):919-23.
106. Auricchio A, Stellbrink C, Sack S, Block M, Vogt J, Bakker P, et al. Long-term clinical effect of hemodynamically optimized cardiac resynchronization therapy in patients with heart failure and ventricular conduction delay. J Am Coll Cardiol 2002;39(12):2026-33.
107. Salukhe TV, Francis DP, Sutton R. Comparison of medical therapy, pacing and defibrillation in heart failure (COMPANION) trial terminated early; combined biventricular pacemaker-defibrillators reduce all-cause mortality and hospitalization. Int J Cardiol 2003;87(2-3):119-20.
108. Cazeau S, Ritter P, Bakdach S, Lazarus A, Limousin M, Henao L, et al. Four chamber pacing in dilated cardiomyopathy. Pacing Clin Electrophysiol 1994;17(11 Pt 2):1974-9.
109. Cazeau S, Ritter P, Lazarus A, Gras D, Backdach H, Mundler O, et al. Multisite pacing for end-stage heart failure: early experience. Pacing Clin Electrophysiol 1996;19(11 Pt 2):1748-57.
110. Abraham WT, Fisher WG, Smith AL, Delurgio DB, Leon AR, Loh E, et al. Cardiac resynchronization in chronic heart failure. N Engl J Med 2002;346(24):1845-53.
111. Cazeau S, Leclercq C, Lavergne T, Walker S, Varma C, Linde C, et al. Effects of multisite biventricular pacing in patients with heart failure and intraventricular conduction delay. N Engl J Med 2001;344(12):873-80.
112. Young JB, Abraham WT, Smith AL, Leon AR, Lieberman R, Wilkoff B, et al. Combined cardiac resynchronization and implantable cardioversion defibrillation in advanced chronic heart failure: the MIRACLE ICD Trial. Jama 2003;289(20):2685-94.
113. Cleland JG, Daubert JC, Erdmann E, Freemantle N, Gras D, Kappenberger L, et al. The effect of cardiac resynchronization on morbidity and mortality in heart failure. N Engl J Med 2005;352(15):1539-49.
114. Yu CM, Bleeker GB, Fung JW, Schalij MJ, Zhang Q, van der Wall EE, et al. Left ventricular reverse remodeling but not clinical improvement predicts long-term survival after cardiac resynchronization therapy. Circulation 2005;112(11):1580-6.
115. St John Sutton MG, Plappert T, Abraham WT, Smith AL, DeLurgio DB, Leon AR, et al. Effect of cardiac resynchronization therapy on left ventricular size and function in chronic heart failure. Circulation 2003;107(15):1985-90.

116. Alonso C, Leclercq C, Victor F, Mansour H, de Place C, Pavin D, et al. Electrocardiographic predictive factors of long-term clinical improvement with multisite biventricular pacing in advanced heart failure. Am J Cardiol 1999;84(12):1417-21.
117. Lunati M, Paolucci M, Oliva F, Frigerio M, Magenta G, Cattafi G, et al. Patient selection for biventricular pacing. J Cardiovasc Electrophysiol 2002;13(1 Suppl):S63-7.
118. Reuter S, Garrigue S, Barold SS, Jais P, Hocini M, Haissaguerre M, et al. Comparison of characteristics in responders versus nonresponders with biventricular pacing for drug-resistant congestive heart failure. Am J Cardiol 2002;89(3):346-50.
119. Reuter S, Garrigue S, Bordachar P, Hocini M, Jais P, Haissaguerre M, et al. Intermediate-term results of biventricular pacing in heart failure: correlation between clinical and hemodynamic data. Pacing Clin Electrophysiol 2000;23(11 Pt 2):1713-7.
120. Stellbrink C, Breithardt OA, Franke A, Sack S, Bakker P, Auricchio A, et al. Impact of cardiac resynchronization therapy using hemodynamically optimized pacing on left ventricular remodeling in patients with congestive heart failure and ventricular conduction disturbances. J Am Coll Cardiol 2001;38(7):1957-65.
121. Yu CM, Lin H, Zhang Q, Sanderson JE. High prevalence of left ventricular systolic and diastolic asynchrony in patients with congestive heart failure and normal QRS duration. Heart 2003;89(1):54-60.
122. Leclercq C, Faris O, Tunin R, Johnson J, Kato R, Evans F, et al. Systolic improvement and mechanical resynchronization does not require electrical synchrony in the dilated failing heart with left bundle-branch block. Circulation 2002;106(14):1760-3.
123. O'Cochlain B, Delurgio D, Leon A, Langberg J. The effect of variation in the interval between right and left ventricular activation on paced QRS duration. Pacing Clin Electrophysiol 2001;24(12):1780-2.
124. Ricci R, Pignalberi C, Ansalone G, Jannone E, Vaccaro MV, Denaro A, et al. Early and late QRS morphology and width in biventricular pacing: relationship to lead site and electrical remodeling. J Interv Card Electrophysiol 2002;6(3):279-85.
125. Vogt J, Krahnefeld O, Lamp B, Hansky B, Kirkels H, Minami K, et al. Electrocardiographic remodeling in patients paced for heart failure. Am J Cardiol 2000;86(9 Suppl 1):K152-K156.
126. Blanc JJ, Etienne Y, Gilard M, Mansourati J, Munier S, Boschat J, et al. Evaluation of different ventricular pacing sites in patients with severe heart failure: results of an acute hemodynamic study. Circulation 1997;96(10):3273-7.
127. Bordachar P, Garrigue S, Reuter S, Hocini M, Kobeissi A, Gaggini G, et al. Hemodynamic assessment of right, left, and biventricular pacing by peak endocardial acceleration and echocardiography in patients with end-stage heart failure. Pacing Clin Electrophysiol 2000;23(11 Pt 2):1726-30.
128. Etienne Y, Mansourati J, Gilard M, Valls-Bertault V, Boschat J, Benditt DG, et al. Evaluation of left ventricular based pacing in patients with congestive heart failure and atrial fibrillation. Am J Cardiol 1999;83(7):1138-40, A9.
129. Etienne Y, Mansourati J, Touiza A, Gilard M, Bertault-Valls V, Guillo P, et al. Evaluation of left ventricular function and mitral regurgitation during left ventricular-based pacing in patients with heart failure. Eur J Heart Fail 2001;3(4):441-7.

130. Le Rest C, Couturier O, Turzo A, Guillo P, Bizais Y, Etienne Y, et al. Use of left ventricular pacing in heart failure: evaluation by gated blood pool imaging. J Nucl Cardiol 1999;6(6):651-6.
131. Touiza A, Etienne Y, Gilard M, Fatemi M, Mansourati J, Blanc JJ. Long-term left ventricular pacing: assessment and comparison with biventricular pacing in patients with severe congestive heart failure. J Am Coll Cardiol 2001;38(7):1966-70.
132. Breithardt OA, Stellbrink C, Franke A, Auricchio A, Huvelle E, Sack S, et al. Echocardiographic evidence of hemodynamic and clinical improvement in patients paced for heart failure. Am J Cardiol 2000;86(9 Suppl 1):K133-K137.
133. Breithardt OA, Stellbrink C, Franke A, Balta O, Diem BH, Bakker P, et al. Acute effects of cardiac resynchronization therapy on left ventricular Doppler indices in patients with congestive heart failure. Am Heart J 2002;143(1):34-44.
134. Breithardt OA, Stellbrink C, Kramer AP, Sinha AM, Franke A, Salo R, et al. Echocardiographic quantification of left ventricular asynchrony predicts an acute hemodynamic benefit of cardiac resynchronization therapy. J Am Coll Cardiol 2002;40(3):536-45.
135. Chamoun AJ, Lenihan DJ, McCulloch M, Ahmad M, Sheahan RG. Resynchronization therapy in dilated cardiomyopathy: confirmation of hemodynamic improvement with real-time three-dimensional echocardiography. Circulation 2001;103(19):E98-8.
136. Curry CW, Nelson GS, Wyman BT, Declerck J, Talbot M, Berger RD, et al. Mechanical dyssynchrony in dilated cardiomyopathy with intraventricular conduction delay as depicted by 3D tagged magnetic resonance imaging. Circulation 2000;101(1):E2.
137. Garrigue S, Jais P, Espil G, Labeque JN, Hocini M, Shah DC, et al. Comparison of chronic biventricular pacing between epicardial and endocardial left ventricular stimulation using Doppler tissue imaging in patients with heart failure. Am J Cardiol 2001;88(8):858-62.
138. Kawaguchi M, Murabayashi T, Fetics BJ, Nelson GS, Samejima H, Nevo E, et al. Quantitation of basal dyssynchrony and acute resynchronization from left or biventricular pacing by novel echo-contrast variability imaging. J Am Coll Cardiol 2002;39(12):2052-8.
139. Kim WY, Sogaard P, Mortensen PT, Jensen HK, Pedersen AK, Kristensen BO, et al. Three dimensional echocardiography documents haemodynamic improvement by biventricular pacing in patients with severe heart failure. Heart 2001;85(5):514-20.
140. Popovic ZB, Grimm RA, Perlic G, Chinchoy E, Geraci M, Sun JP, et al. Noninvasive assessment of cardiac resynchronization therapy for congestive heart failure using myocardial strain and left ventricular peak power as parameters of myocardial synchrony and function. J Cardiovasc Electrophysiol 2002;13(12):1203-8.
141. Prinzen FW, Hunter WC, Wyman BT, McVeigh ER. Mapping of regional myocardial strain and work during ventricular pacing: experimental study using magnetic resonance imaging tagging. J Am Coll Cardiol 1999;33(6):1735-42.
142. Sogaard P, Egeblad H, Kim WY, Jensen HK, Pedersen AK, Kristensen BO, et al. Tissue Doppler imaging predicts improved systolic performance and reversed left ventricular remodeling during long-term cardiac resynchronization therapy. J Am Coll Cardiol 2002;40(4):723-30.

143. Sogaard P, Egeblad H, Pedersen AK, Kim WY, Kristensen BO, Hansen PS, et al. Sequential versus simultaneous biventricular resynchronization for severe heart failure: evaluation by tissue Doppler imaging. Circulation 2002;106(16):2078-84.
144. Sogaard P, Kim WY, Jensen HK, Mortensen P, Pedersen AK, Kristensen BO, et al. Impact of acute biventricular pacing on left ventricular performance and volumes in patients with severe heart failure. A tissue doppler and three-dimensional echocardiographic study. Cardiology 2001;95(4):173-82.
145. Sohn DW, Chai IH, Lee DJ, Kim HC, Kim HS, Oh BH, et al. Assessment of mitral annulus velocity by Doppler tissue imaging in the evaluation of left ventricular diastolic function. J Am Coll Cardiol 1997;30(2):474-80.
146. Wyman BT, Hunter WC, Prinzen FW, Faris OP, McVeigh ER. Effects of single- and biventricular pacing on temporal and spatial dynamics of ventricular contraction. Am J Physiol Heart Circ Physiol 2002;282(1):H372-9.
147. Yu CM, Chau E, Sanderson JE, Fan K, Tang MO, Fung WH, et al. Tissue Doppler echocardiographic evidence of reverse remodeling and improved synchronicity by simultaneously delaying regional contraction after biventricular pacing therapy in heart failure. Circulation 2002;105(4):438-45.
148. Auricchio A, Ding J, Spinelli JC, Kramer AP, Salo RW, Hoersch W, et al. Cardiac resynchronization therapy restores optimal atrioventricular mechanical timing in heart failure patients with ventricular conduction delay. J Am Coll Cardiol 2002;39(7):1163-9.
149. Butter C, Auricchio A, Stellbrink C, Fleck E, Ding J, Yu Y, et al. Effect of resynchronization therapy stimulation site on the systolic function of heart failure patients. Circulation 2001;104(25):3026-9.
150. Kass DA, Chen CH, Curry C, Talbot M, Berger R, Fetics B, et al. Improved left ventricular mechanics from acute VDD pacing in patients with dilated cardiomyopathy and ventricular conduction delay. Circulation 1999;99(12):1567-73.
151. Leclercq C, Walker S, Linde C, Clementy J, Marshall AJ, Ritter P, et al. Comparative effects of permanent biventricular and right-univentricular pacing in heart failure patients with chronic atrial fibrillation. Eur Heart J 2002;23(22):1780-7.
152. Leon AR, Greenberg JM, Kanuru N, Baker CM, Mera FV, Smith AL, et al. Cardiac resynchronization in patients with congestive heart failure and chronic atrial fibrillation: effect of upgrading to biventricular pacing after chronic right ventricular pacing. J Am Coll Cardiol 2002;39(8):1258-63.
153. Linde C, Leclercq C, Rex S, Garrigue S, Lavergne T, Cazeau S, et al. Long-term benefits of biventricular pacing in congestive heart failure: results from the MUltisite STimulation in cardiomyopathy (MUSTIC) study. J Am Coll Cardiol 2002;40(1):111-8.
154. Beshai JF, Grimm RA, Nagueh SF, Baker JH, 2nd, Beau SL, Greenberg SM, et al. Cardiac-resynchronization therapy in heart failure with narrow QRS complexes. N Engl J Med 2007;357(24):2461-71.
155. Chung ES, Leon AR, Tavazzi L, Sun JP, Nihoyannopoulos P, Merlino J, et al. Results of the Predictors of Response to CRT (PROSPECT) trial. Circulation 2008;117(20):2608-16.

156. Yu CM, Abraham WT, Bax J, Chung E, Fedewa M, Ghio S, et al. Predictors of response to cardiac resynchronization therapy (PROSPECT)--study design. Am Heart J 2005;149(4):600-5.